Precambrian Research 317 (2018) 14–32

Contents lists available at ScienceDirect

Precambrian Research

journal homepage: www.elsevier.com/locate/precamres

Paleomagnetism, magnetic anisotropy and U-Pb baddeleyite geochronology of the early Neoproterozoic Blekinge-Dalarna dolerite dykes, Sweden

Zheng Gong[a,*], David A.D. Evans[a], Sten-Åke Elming[b], Ulf Söderlund[c,d], Johanna M. Salminen[e]

[a] Department of Geology and Geophysics, Yale University, 210 Whitney Avenue, New Haven, CT 06511, USA
[b] Department of Civil, Environmental and Natural Resources Engineering, Luleå University of Technology, SE-971 87 Luleå, Sweden
[c] Department of Geology, Lund University, SE-223 62 Lund, Sweden
[d] Swedish Museum of Natural History, Laboratory of Isotope Geology, SE-104 05 Stockholm, Sweden
[e] Department of Geosciences and Geography, University of Helsinki, Helsinki 00014, Finland

ARTICLE INFO

Keywords:
Blekinge-Dalarna dolerite (BDD) dykes
Sveconorwegian loop
Baltica
Paleomagnetism
Magnetic anisotropy
U-Pb baddeleyite geochronology

ABSTRACT

Paleogeographic proximity of Baltica and Laurentia in the supercontinent Rodinia has been widely accepted. However, robust paleomagnetic poles are still scarce, hampering quantitative tests of proposed relative positions of the two cratons. A recent paleomagnetic study of the early Neoproterozoic Blekinge-Dalarna dolerite (BDD) dykes in Sweden provided a 946–935 Ma key pole for Baltica, but earlier studies on other BDD dykes discerned large variances in paleomagnetic directions that appeared to indicate more complicated motion of Baltica, or alternatively, unusual geodynamo behavior in early Neoproterozoic time. We present combined paleomagnetic, rock magnetic, magnetic fabric and geochronological studies on BDD dykes in the Dalarna region, southern Sweden. Positive baked-contact and paleosecular variation tests support the reliability of the 951–935 Ma key pole (Plat = −2.6°N, Plon = 239.6°E, A_{95} = 5.8°, N = 12 dykes); and the ancient magnetic field was likely a stable geocentric axial dipole at that time, based on a positive reversal test. Detailed analysis of the 947 Ma Nornäs dyke, one of the dykes previously showing anomalous directions, suggests a partial viscous remagnetization. Therefore, the observed large variances in nearly coeval BDD dykes are suspected to result from present-day overprints that were not adequately removed in earlier studies. In addition, we obtained a 971 Ma virtual geomagnetic pole (Plat = −27.0°N, Plon = 230.4°E, A_{95} = 14.9°, N = 4 dykes) for Baltica. Comparing similar-aged poles from Laurentia, we suggest that Baltica and Laurentia drifted together from high to low latitude between 970–960 Ma and 950–935 Ma, and returned back to high latitude by 920–870 Ma. In this scenario, the apparent polar wander paths of Baltica and Laurentia may be more complicated than the previously proposed, solitary Sveconorwegian and Grenville loops. The new U-Pb baddeleyite ages do not support BDD dykes as a giant circumferential swarm generated by a mantle plume, and the prolonged timespan of dyke intrusion is likely associated with the plate boundary forces as causing gravitational extension at the waning stage of the Sveconorwegian orogeny.

1. Introduction

Although the existence of the Proterozoic supercontinent Rodinia has long been suggested, its configuration is still highly debated, and new studies continue to paint different pictures regarding the shape of Rodinia (e.g., Slagstad et al., 2013; Wen et al., 2017; Wen et al., 2018). Nonetheless, the juxtaposition of Laurentia and Baltica in Rodinia is widely adopted in various reconstruction models (e.g., Dalziel, 1997; Pisarevsky et al., 2003; Cawood and Pisarevsky, 2006; Li et al., 2008; Evans, 2009), in order to account for geological similarities between the two cratons. As the only quantitative method to constrain the paleolatitude and the orientation of pre-Pangea continents, paleomagnetism plays an important role in testing current reconstruction models of Laurentia and Baltica. The apparent polar wander (APW) paths of Laurentia and Baltica, including the Grenville and Sveconorwegian loops, respectively, show a broad agreement during post-1.0-Ga Rodinia assembly (Li et al., 2008), supporting the paleogeographic proximity of the two cratons. However, most paleomagnetic poles on the Grenville and Sveconorwegian loops derive from high-grade metamorphic rocks, making the determination of the age of remanence acquisition difficult (Brown and McEnroe, 2012; Brown and McEnroe, 2015). Compilation of paleomagnetic poles with ages

* Corresponding author.
E-mail address: z.gong@yale.edu (Z. Gong).

https://doi.org/10.1016/j.precamres.2018.08.019
Received 22 May 2018; Received in revised form 22 August 2018; Accepted 25 August 2018
Available online 28 August 2018
0301-9268/

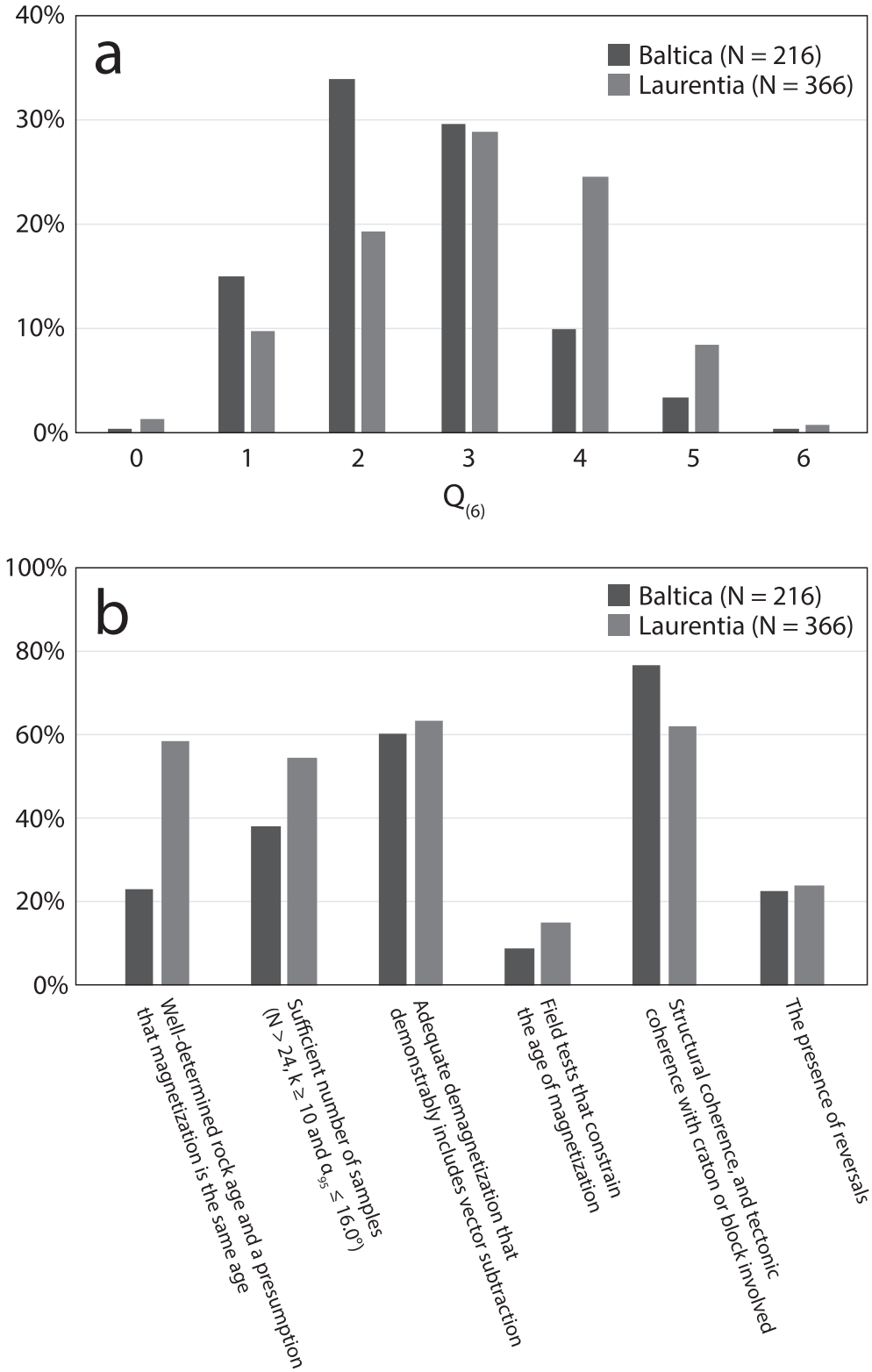

Fig. 1. Compilation of paleomagnetic poles from Baltica and Laurentia within the 1.3–0.9 Ga interval (Veikkolainen et al., 2017). (a) Sum of quality criteria $Q_{(6)}$ (Van der Voo, 1990), excluding the seventh criterion as in the Precambrian paleomagnetism database PALEOMAGIA. (b) Individual quality criteria (Van der Voo, 1990). N = number of paleomagnetic poles.

between 1.3 Ga and 0.9 Ga (Veikkolainen et al., 2017) shows that even though numerous poles have been generated for Baltica and Laurentia, high-quality poles with quality criteria Q_{Voo} value larger than 4 are scarce (Fig. 1a), and most poles have no field tests to constrain the age of remanence (Fig. 1b). As a result, large uncertainties remain regarding the shapes and younging directions of the Grenville and Sveconorwegian loops (Hyodo and Dunlop, 1993; Elming et al., 1993; Weil et al., 2006; Elming et al., 2014).

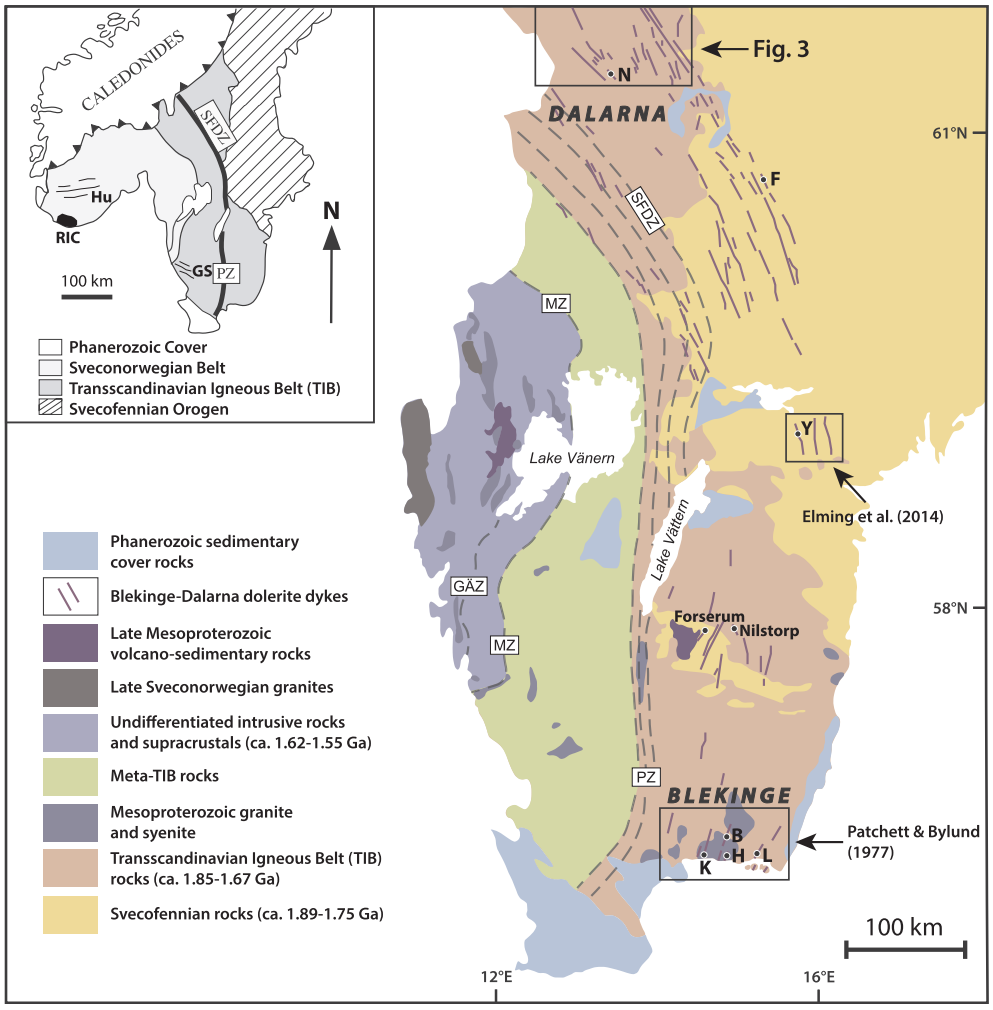

Fig. 2. Geologic map of southern Sweden. GÄZ = Göta Älv Zone, MZ = Mylonite Zone, PZ = Protogine Zone, SFDZ = Sveconorwegian Frontal Deformation Zone. Inset map shows the major tectonic divisions of southern Sweden (modified from Söderlund et al., 2004b). GS = Göteborg-Slussen dykes, Hu = Hunnedalen dykes, RIC = Rogaland Igneous Complex. Small boxes show the locations of Y1, Y2 (Y), and Falun (F) dykes in Elming et al. (2014); and Lösen-Fäjö (L), Bräkne-Hoby (B), Karlshamn (K), and Härsjön (H) dykes in Patchett and Bylund (1977); and Nornäs dyke (N) in this study.

Mafic intrusions are promising targets for yielding high-quality poles since they are usually enriched in magnetite grains. Also, baddeleyite grains in mafic intrusions can be directly dated by U-Pb method with high precision (Söderlund et al., 2005). A recent study of the Blekinge-Dalarna dolerite (BDD) dykes in southern Sweden generated a 946–935 Ma low-latitude pole that has been proposed as a key pole for Baltica (Elming et al., 2014). However, earlier studies of BDD dykes show large variances in paleomagnetic directions (Patchett and Bylund, 1977; Bylund, 1985; Bylund and Elming, 1992) that might indicate unusual cratonic motions or complicated geomagnetic behavior. Here we present detailed paleomagnetic, rock magnetic and magnetic fabric studies on a number of BDD dykes in the Dalarna region, southern Sweden, in order to better understand the paleogeography of Baltica in early Neoproterozoic time. We also present new U-Pb baddeleyite ages that shed light on the tectonic origin of BDD dykes.

2. Geologic background, previous work and sampling

Following the Svecofennian orogeny (2.0–1.75 Ga), Baltica grew outward as a result of accretionary tectonics manifested by the 1.81–1.76 Ga Transscandinavian Igneous Belt (TIB; Bogdanova et al., 2015). Afterwards, there was a protracted interval of mafic magmatism peaked at 1.6 Ga, 1.57 Ga, 1.47–1.44 Ga, 1.27–1.26 Ga, 1.22 Ga, and 0.98–0.95 Ga, respectively (Söderlund et al., 2005; Brander and Söderlund, 2009). The 1.47–1.44 Ga magmatism, referred to as the Danopolonian event (Bogdanova et al., 2001), is largely coeval with dynamic high-grade metamorphism in southwestern Sweden, and is suggested to be related to convergent active margin processes called the Hallandian event (Christoffel et al., 1999; Söderlund et al., 2002; Möller et al., 2007; Brander and Söderlund, 2009). After the Hallandian event, the 1.1–0.9 Ga Sveconorwegian orogeny (e.g., Bingen et al., 2008) extensively reworked the basement rocks west of the Protogine Zone (PZ) and the Sveconorwegian Frontal Deformation Zone (SFDZ) in southwest Scandinavia (Fig. 2; Wahlgren et al., 1994). Later, Caledonian allochthons were thrust onto the northwest margin of Baltica at 0.6–0.4 Ga (Fig. 2; Gaál and Gorbatschev, 1987; Bingen and Solli, 2009).

Partly coincident with the Sveconorwegian orogeny, the early Neoproterozoic BDD dykes intruded the TIB and Svecofennian rocks east of the PZ and SFDZ, over an extent of 750 km (Fig. 2). One prominent feature of BDD dykes is their arcuate shape, trending NE-SW in the Blekinge region, and deflected ~60° to NW-SE in the Dalarna region (Fig. 2). The ages of BDD dykes are well established by U-Pb baddeleyite geochronology and $^{40}Ar/^{39}Ar$ whole-rock dating, ranging from 978 Ma to 939 Ma (Söderlund et al., 2005; Elming et al., 2014). The origin of BDD dykes is debated. Different models have been proposed, including fracturing due to late Sveconorwegian uplift (Patchett

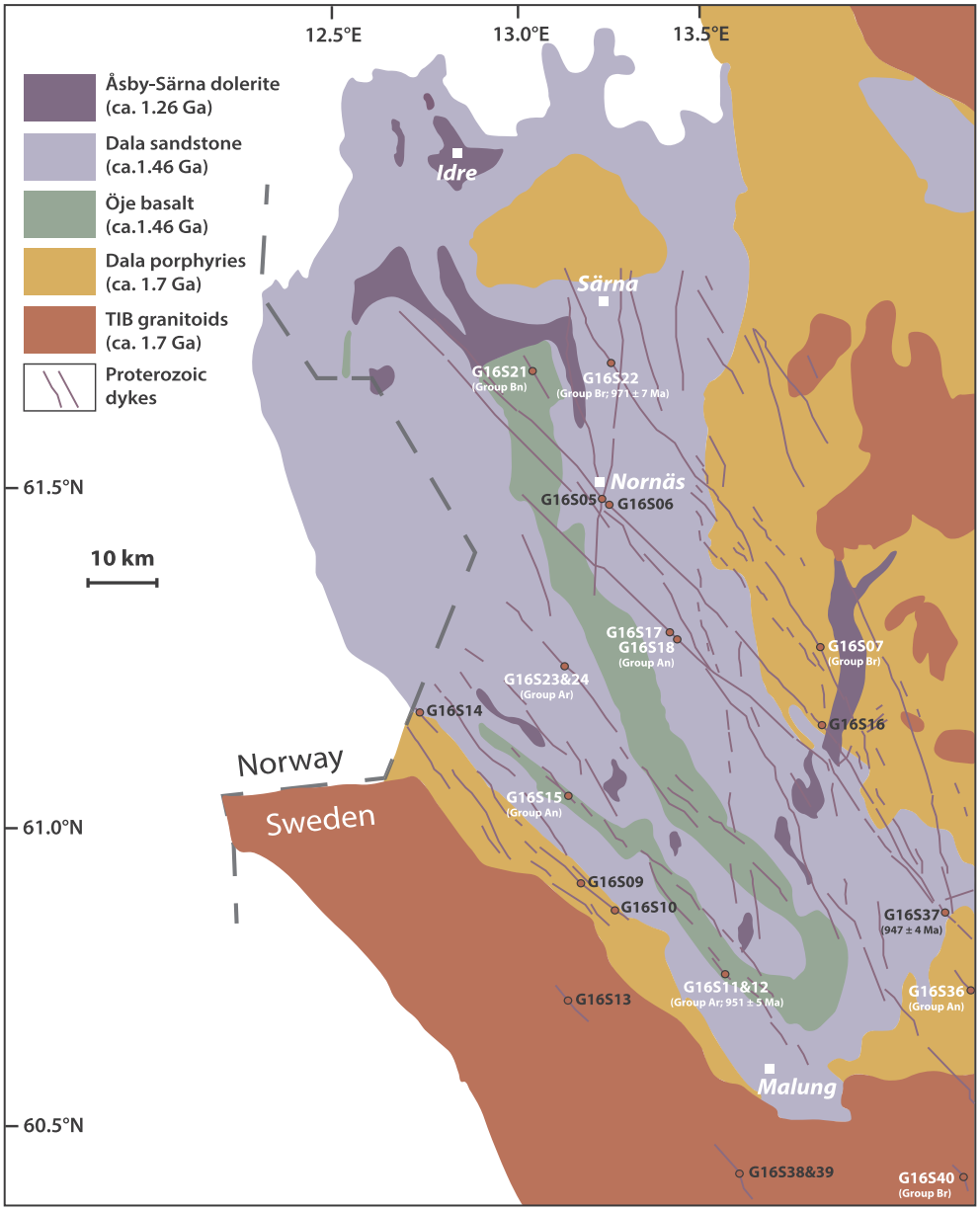

Fig. 3. Geologic map of the western Dalarna region (modified from Lundmark and Lamminen, 2016). Proterozoic dyke locations are based on Ripa et al. (2012). Sites yield interpretable paleomagnetic results (white) and sites give paleomagentically unstable directions/partial remagnetization (black) are differentiated by color.

and Bylund, 1977), gravitational collapse at the final stage of the Sveconorwegian orogeny (Pisarevsky and Bylund, 2006), and the giant circumferential system of a mantle plume (Buchan and Ernst, 2016). Petrological studies show that BDD dykes are fine- to medium-grained with slight alteration, and the major minerals consist of plagioclase, olivine, clinopyroxene, orthopyroxene, biotite, ilmenite, and titanomagnetite (Johansson and Johansson, 1990; Solyom et al., 1992).

Previous paleomagnetic work focused on the southern and central part of BDD dykes (e.g., Patchett and Bylund, 1977; Bylund, 1985; Bylund and Elming, 1992), while the northern part is relatively less studied. Recently, Elming et al. (2014) proposed a low-latitude pole for Baltica at 946–935 Ma, combining the results of several BDD dykes in the Norrköping and Falun areas with the 935 Ma Göteborg-Slussen dykes in southwestern Sweden (Fig. 2; Pisarevsky and Bylund, 2006). The reliability of this low-latitude pole is supported by a positive baked-contact test and the appearance of antipodal directions. However, large variances still remain in the paleomagnetic results of BDD dykes, complicating the application of this low-latitude pole to paleogeographic reconstruction of Baltica. For example, the 947 Ma Nornäs dyke yields a high-latitude pole (Piper and Smith, 1980; Bylund, 1985), which apparently contradicts with the result of Elming et al. (2014). It is also difficult to explain their difference by plate tectonics because they are very similar in age and would imply extremely rapid continental motions. Alternative interpretations have been suggested, such as late-stage selective remagnetization, true polar wander, a non-dipole geomagnetic field or the non-averaged paleosecular variation (Pesonen

Table 1
Results of U-Pb baddeleyite geochronology.

Sample (number of grains)	U/Th	Pb_c/Pb_{tot}[1]	$^{206}Pb/^{204}Pb$	$^{207}Pb/^{235}U$	± 2 s% Error	$^{206}Pb/^{238}U$	± 2 s% Error	$^{207}Pb/^{235}U$	$^{206}Pb/^{238}U$	$^{207}Pb/^{206}Pb$	± 2σ	Concordance
			[Raw][2]	[Corr][3]				[Age, Ma]				
G16S12												
Bd-1 (2 grains)	27.4	0.085	818.2	1.5298	1.15	0.15711	1.10	942.4	940.7	946.5	9.2	0.994
Bd-2 (4 grains)	14.3	0.046	1449.3	1.5358	0.61	0.15707	0.51	944.8	940.4	955.1	7.0	0.985
Bd-3 (3 grains)	7.3	0.174	375.2	1.5337	1.90	0.15753	1.82	944.0	943.1	946.1	15.4	0.997
G16S22												
Bd-1 (2 grains)	5.9	0.311	214.3	1.5922	3.96	0.16185	3.75	967.2	967.1	967.4	33.6	1.000
Bd-2 (5 grains)	12.3	0.080	820.0	1.5437	0.82	0.15688	0.73	948.0	939.4	968.0	8.4	0.970
Bd-3 (5 grains)	9.0	0.168	365.5	1.5875	1.12	0.16072	0.99	965.3	960.8	975.8	11.6	0.985
G16S37												
Bd-1 (1 grain)	13.0	0.033	2026.6	1.5314	0.41	0.15714	0.33	943.0	940.8	948.2	5.2	0.992
Bd-2 (2 grains)	17.1	0.070	947.4	1.5281	0.74	0.15656	0.68	941.7	937.6	951.4	6.9	0.986
Bd-3 (2 grains)	7.6	0.119	520.8	1.5312	0.72	0.15773	0.65	943.0	944.1	940.3	7.0	1.004

[1] Pb_c = common Pb, Pb_{tot} = total Pb (radiogenic + blank + initial).
[2] Measured ratio, corrected for fractionation and spike.
[3] Isotopic ratios corrected for fractionation (0.1% per amu for Pb), spike contribution, blank (0.4 pg Pb and 0.04 pg U), and initial common Pb. Initial common Pb corrected with isotopic compositions from the model of Stacey and Kramers (1975) at the age of the sample.

and Klein, 2013). However, none of these has been fully examined. Notably, the result of the Nornäs dyke was obtained more than three decades ago when modern laboratory treatment and data analysis of paleomagnetism had not been fully developed. Hence, it is necessary to restudy the Nornäs dyke with more detailed and sophisticated techniques.

Since more than 90% of the bedrock in the Dalarna region is covered by glacial deposits, aeromagnetic data (Ripa et al., 2012) and data from geological mapping of the Swedish Geological Survey (Ripa, personal communication) were used to help delineate dykes in the field. For detailed mapping of the outcrops, a portable magnetic susceptibility meter was used to determine the extension of the dykes and contacts to host rocks. A number of NW-SE trending dykes in the Dalarna region were sampled using a portable gasoline-powered rock drill (Fig. 3). Host rocks (ca. 1.46 Ga Öje basalt and ca. 1.46 Ga Dala sandstone) were collected in two sites for baked-contact tests, the former where a clear intrusive contact was observed, and the latter where the concealed contact could be triangulated to within about a meter of the baked host-rock samples. Core samples were oriented with a Brunton compass, and sun-compass readings were also taken in order to correct any small-scale magnetic anomaly in the outcrop. Block samples were collected from the central parts of dykes for U-Pb baddeleyite geochronology.

3. Methods

3.1. U-Pb baddeleyite geochronology

All samples were crushed, and baddeleyite grains were separated using the Wilfley table technique following Söderlund and Johansson (2002) at Lund University in Sweden. The extracted baddeleyite grains are dark to moderately brown. Grains from all samples are fresh without any trace of alteration. About 1–5 grains per fraction were combined and transferred to clean Teflon capsules. Grains were washed in numerous steps using 3 M HNO_3, including one step on a hotplate (~30 min). One drop of the ^{205}Pb-$^{233-236}U$ tracer solution and 10 drops of HF-HNO_3 (10:1) were added to each capsule. Baddeleyite grains were completely dissolved after 3 days in an oven under high pressure at a temperature of ~190°C. The samples were evaporated on a hotplate and then dissolved in 10 drops of 6.2 M HCl. One drop of 0.25 M H_3PO_4 was added to each capsule before it dried down. U and Pb were loaded on an outgassed Re filament together with a small amount of silica gel.

Thermal Ionization Mass Spectrometry (TIMS) was performed at the Laboratory of Isotope Geology at the Swedish Museum of Natural History in Stockholm, Sweden, using a Thermo Finnigan Triton TIMS system. An ETP SEM detector equipped with a RPQ filter was used to measure the Pb and U isotope intensities in dynamic (peak-switching) mode. Pb-isotopes were measured at a filament temperature in the 1200–1230°C range, while U-isotopes were measured in dynamic mode on the SEM with filament temperatures exceeding 1300°C. Data reduction was performed using the Excel add-in "Isoplot" of Ludwig (2003); decay constants for ^{238}U and ^{235}U follow those of Jaffey et al. (1971). All errors in age and isotopic ratios are quoted at 2σ. Initial Pb isotope compositions were corrected according to the global common Pb evolution model of Stacey and Kramers (1975). U-Pb data are presented in Table 1 and the fractions are plotted in the concordia diagrams in Fig. 4.

3.2. Magnetic measurements

Magnetic measurements were conducted in the Paleomagnetic Laboratory and Archaeomagnetism Laboratory at Yale University, USA. In order to understand the pattern of dyke propagation and to discern the possible alteration or deformation of dykes (Hrouda, 1982; Rochette et al., 1992), anisotropy of magnetic susceptibility (AMS) was measured for each dyke using an AGICO Kappabridge KLY-4S susceptibility meter. AMS data were analyzed in Anisoft42 software. To characterize magnetic mineralogy, representative samples were subjected to thermomagnetic susceptibility analysis. Temperature ranges from 25°C to 700°C and is controlled by a CS3 high temperature furnace apparatus. Bulk magnetic susceptibility was measured during heating and cooling in an argon gas environment in order to subdue magnetic phase transition. Magnetic grain size was inferred by the Day plot (Day et al., 1977) constructed by magnetic parameters, which are determined by hysteresis loop measurement using a MicroMag 2900 alternating gradient magnetometer (AGM). After the measurement of natural

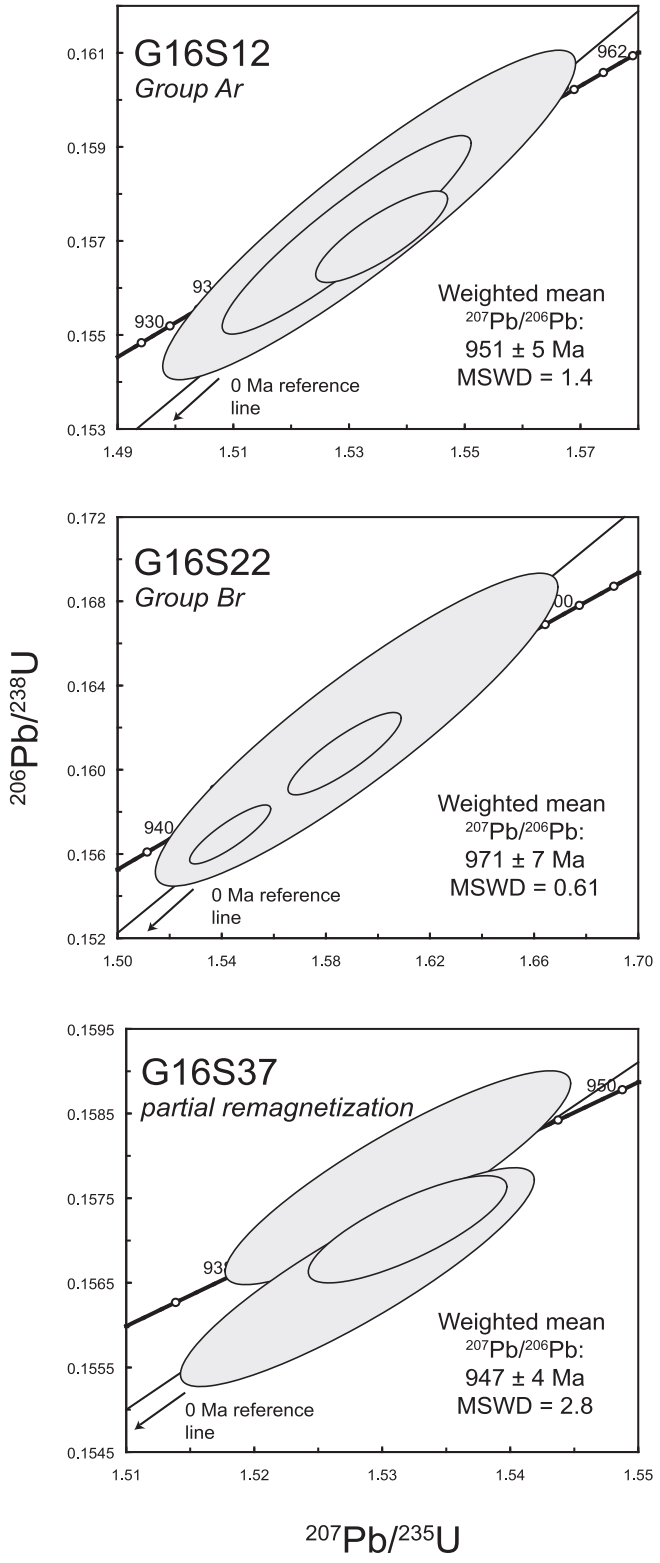

Fig. 4. U-Pb concordia diagrams of dated BDD dykes.

remanent magnetization (NRM), samples were cooled to liquid nitrogen temperature (~77 K) in a magnetic shielded container to demagnetize the remanence carried by multidomain grains (Muxworthy and McClelland, 2000). Thermal demagnetization was conducted in an ASC Scientific TD-48 thermal demagnetizer with stepwise heating up to 580°C in 15–20 steps in a nitrogen gas environment. Sister samples from each dyke were demagnetized using alternating field (AF) in a Molspin tumbler demagnetizer. After each thermal or AF demagnetization step, remanence was measured by a 2G Enterprises cryogenic DC-SQuID magnetometer with an automatic sample-changing device (Kirschvink et al., 2008). Paleomagnetic vectors were calculated using principal component analysis (Kirschvink, 1980) and the great circle method (McFadden and McElhinny, 1988), and were plotted using vector-endpoint diagrams (Zijderveld, 1967) in PaleoMag X software (Jones, 2002). Paleogeographic reconstruction was carried out using GPlates software (Boyden et al., 2011).

4. Results

4.1. U-Pb baddeleyite geochronology

We report U-Pb baddeleyite TIMS ages of three NW-SE trending BDD dykes from the Dalarna region. Data are summarized in Table 1, and concordia diagrams are shown in Fig. 4. Three baddeleyite fractions of dyke G16S12, which is intrusive into the Öje basalt (G16S11), are concordant at 951 ± 5 Ma (2σ, mean square weighted deviates [MSWD] = 1.4). This age is calculated as the weighted mean of $^{207}Pb/^{206}Pb$ dates for these fractions. Three fractions of dyke G16S22 were analyzed, of which two are concordant within uncertainty whereas one analysis is slightly discordant. The weighted mean of $^{207}Pb/^{206}Pb$ dates is 971 ± 7 Ma (2σ, MSWD = 0.61). Three fractions of dyke G16S37, which is probably the southern extension of the Nornäs dyke, cluster at and just below the concordia curve. The weighted mean is 947 ± 4 Ma (2σ, MSWD = 2.8). These age estimates are interpreted as dating the crystallization of the rocks.

Before this study, a total of 11 ages of BDD dykes/sills were published, with nine U-Pb baddeleyite ages (Söderlund et al., 2004a; Söderlund et al., 2005) and two $^{40}Ar/^{39}Ar$ whole-rock ages (Elming et al., 2014). We provide three new U-Pb baddeleyite ages. Collectively, they demonstrate a ~ 40 million-year range of BDD intrusions with probably three magmatic pulses, extending from 978 Ma to 939 Ma (Fig. 5).

4.2. Rock magnetism

AMS data show that the degree of anisotropy (P_j) of BDD dykes is typically below 6%, which is a common value for primary fabric of igneous rocks (Hrouda, 1982). Low P_j values indicate that these rocks have not experienced significant deformation, hence, have a reasonable chance of retaining primary magnetization. The majority of dykes exhibit oblate fabrics with K_1 and K_2 axes dispersed in the NW-SE oriented, vertical or sub-vertical plane (Fig. 6e). Some dykes show prolate fabrics with K_1 axis pointing to the NW-SE direction (Fig. 6a). The orientation of magnetic anisotropy ellipsoid genuinely reflects the trends (NW-SE) of these dykes (Knight and Walker, 1988), which is also supported by field observations and the aeromagnetic anomaly map (Fig. 3; Ripa et al., 2012). AMS of Öje basalt is expected to have a horizontal oblate fabric; the K_3 axis shows a transition from steep to shallow directions (Fig. 6c). Samples with shallow K_3 axes are close to the contact and the chilled margin of dyke G16S12. It is suspected that some secondary magnetic minerals might grow along the basalt contact zone due to the migration of reducing fluids, and cause anomalously shallow K_3 axis. But the remanences of the secondary magnetic minerals are adequately removed by thermal demagnetization and have no influence on primary paleomagnetic signals (see discussion below). AMS of the Dala

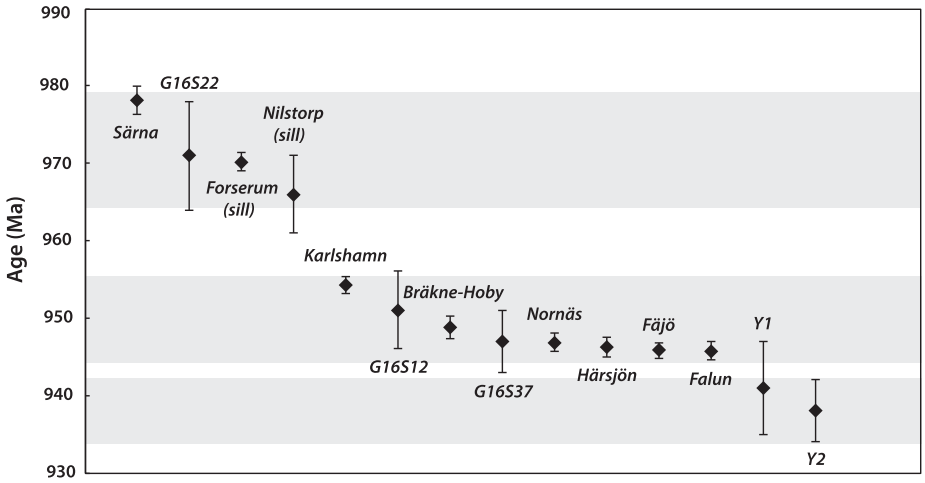

Fig. 5. Summary of ages from 980 Ma to 930 Ma BDD-related intrusions in southern Sweden. Age references are listed in Table 2. Shaded areas show age ranges of possible pulses of BDD intrusions.

sandstone (G16S24) shows a typical depositional fabric (oblate and horizontal), with K_3 axis perpendicular to the bedding plane and K_1 and K_2 axes distributed parallel to the bedding plane (Fig. 6h).

Thermomagnetic susceptibility analysis of BDD dykes shows that heating and cooling curves are generally reversible (Fig. 7). During heating, the magnetic susceptibility decreases substantially between 580°C and 600°C, which provides clear evidence for the presence of magnetite. Minor drops in magnetic susceptibility are also noticed between 600°C and 700°C, indicating small amounts of hematite or maghemite. Exceptions are Öje basalt (G16S11) and dyke G16S12, which yield a distinct susceptibility hump and a large decline between 300°C and 400°C on the heating curve (Fig. 7c-d). This temperature range coincides with the Curie temperature of magnetic sulfides (pyrrhotite or greigite). During heating, the magnetic sulfides were broken down to form new magnetite, as suggested by the sharply increased susceptibility at 580°C on the cooling curve. The magnetic sulfides are likely the reason for shallow K_3 axis observed in the AMS data of Öje basalt (G16S11). Dala sandstone (G16S24) has a low magnetic susceptibility and shows a gradual decrease in susceptibility between 600°C and 700°C (Fig. 7g), suggesting the major magnetic phase is hematite or titano-hematite.

The coercivity of remanence of BDD dykes determined by hysteresis loop measurement is typically less than 30 mT, which is a normal value for magnetite. Only dyke G16S12 gives slightly higher coercivity (~80 mT), showing the contribution from magnetic sulfides (Fig. 8b). The typical grain size of magnetic phases in BDD dykes falls in pseudo-single domain (PSD) region on the Day plot. According to Dunlop (2002)'s theoretical estimates, the magnetic grains are mixtures of single domain (SD) and multidomain (MD) minerals with varying SD content ranging from 20% to 60% (Fig. 8c).

4.3. Paleomagnetism

Paleomagnetic results show that during heating, most samples exhibit a significant decline of remanence at ~580°C, close to the unblocking temperature for pure magnetite (Fig. 9). Samples that were subjected to liquid nitrogen bath show a large decrease of remanence, indicating that the viscous remanence carried by MD grains has been effectively removed (Fig. 9). Some samples show a gradual loss of remanence at lower temperatures, which could be either due to the demagnetization of larger size grains or magnetic sulfides. Most samples yield a clear decay-to-origin component between 500°C and 580°C, which is defined as the characteristic remanent magnetization (ChRM). Only samples from sites G16S17 and G16S18 (two sites were collected from the same dyke) were analyzed by the combination of principal component analysis and great circle method, owing to the overlapping unblocking temperatures of different-sized grains.

Usable paleomagnetic directions of BDD dykes fall into two statistically different groups (Fig. 10a), one with shallower inclinations (Group A) and another with steeper inclinations (Group B). Importantly, the dating results also show that the two groups are different in age. Group A is about 951 ± 5 Ma, ~20 million years younger than Group B (971 ± 7 Ma). Both groups show two polarities. Following Precambrian paleomagnetism database PALEOMAGIA's nomenclature (Veikkolainen et al., 2017), we assign reverse polarity to sites with southeasterly declinations (Groups Ar, Br) and normal polarity to sites with northwesterly declinations (Groups An, Bn; Table 2). Paleomagnetic directions of Group A are resemble those of the Y1, Y2 and Falun dykes obtained in Elming et al. (2014). A positive baked-contact test supports the primary origin of the NW-up direction (Group An; Elming et al., 2014), In addition, we have two positive baked-contact tests for the SE-down direction (Group Ar). The baked areas of the Öje basalt (G16S11) and the Dala sandstone (G16S24), which were intruded by dykes G16S12 and G16S23 respectively, show similar remanence to BDD dykes, but are very different from their primary (unbaked) directions (Piper and Smith, 1980; Fig. 10a). We performed a reversal test on Group A, together with Y1, Y2 and Falun dykes from Elming et al. (2014) and the Tuve, Small, Hjuvik and Slussen dykes from Pisarevsky and Bylund (2006); the test is demonstrated to be positive with classification C (γ/γ_c = 8.7°/13.9°; McFadden and McElhinny, 1990). On the basis of the similar ages and paleomagnetic results of Pisarevsky and Bylund (2006), Elming et al. (2014), and our data, we obtained a new mean 951–935 Ma paleomagnetic pole: Plat = −2.6°N, Plon = 239.6°E, A_{95} = 5.8° (N = 12 dykes; Table 2). There is no baked-contact test for the four dykes in Group B, but their demagnetization patterns, such as the square-shouldered thermal decay curve with the unblocking temperature close to 580°C, suggest that their ChRMs are probably primary (Fig. 9). The number of dykes in Group B is insufficient for the reversal test, but quasi-antipodal directions have been observed, also supporting the notion that dykes in Group B carry

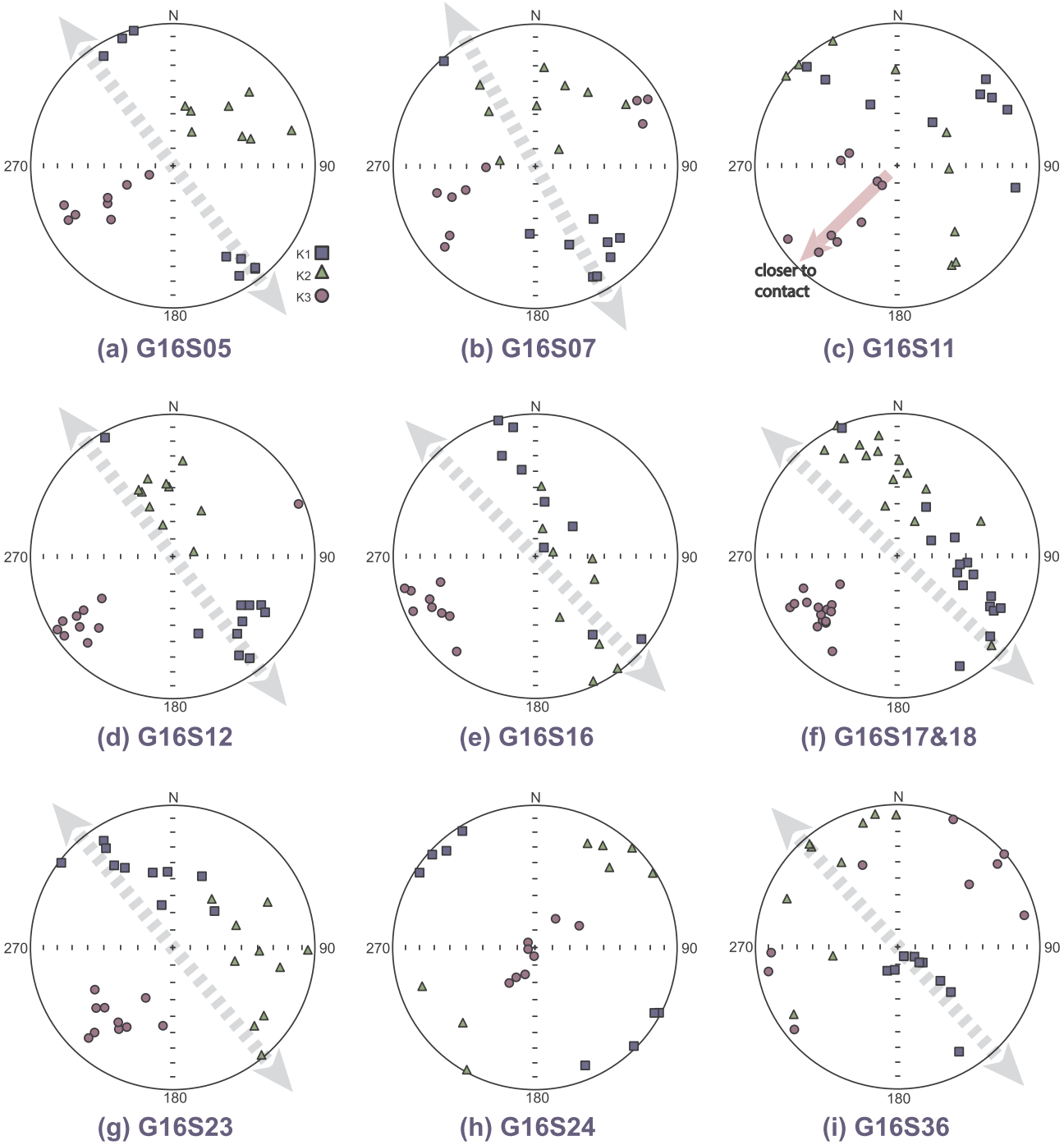

Fig. 6. Representative stereonet projections of the anisotropy of magnetic susceptibility (AMS) data. Squares, triangles and circles show the principal axes of AMS ellipsoids. Grey arrows indicate the trends of dykes inferred from aeromagnetic anomalies (Ripa et al., 2012). Red arrow represents the evolution of AMS ellipsoid of Öje basalt. (For interpretation of the references to colour in this figure legend, the reader is referred to the web version of this article.)

primary remanences. We calculated a 971 Ma virtual geomagnetic pole (VGP) from Group B, which is Plat = −27.0°N, Plon = 230.4°E, A_{95} = 14.9° (N = 4 dykes; Table 2).

Paleomagnetic results of the Nornäs dyke (G16S05 and G16S06; 946.8 ± 1.2 Ma) show that the natural remanent magnetization (NRM) direction is very close to the steep ChRM yielded from previous work (Piper and Smith, 1980; Bylund, 1985). The steep ChRM is also very close to present-day field (PDF) direction (Fig. 10b). However, as temperature or AF intensity increases, the inclination gradually decreases (Fig. 11). It is noteworthy that the direction of remanences of some samples are able to migrate towards the upper hemisphere at ~ 570°C or ~ 30 mT. The remanence becomes unstable when

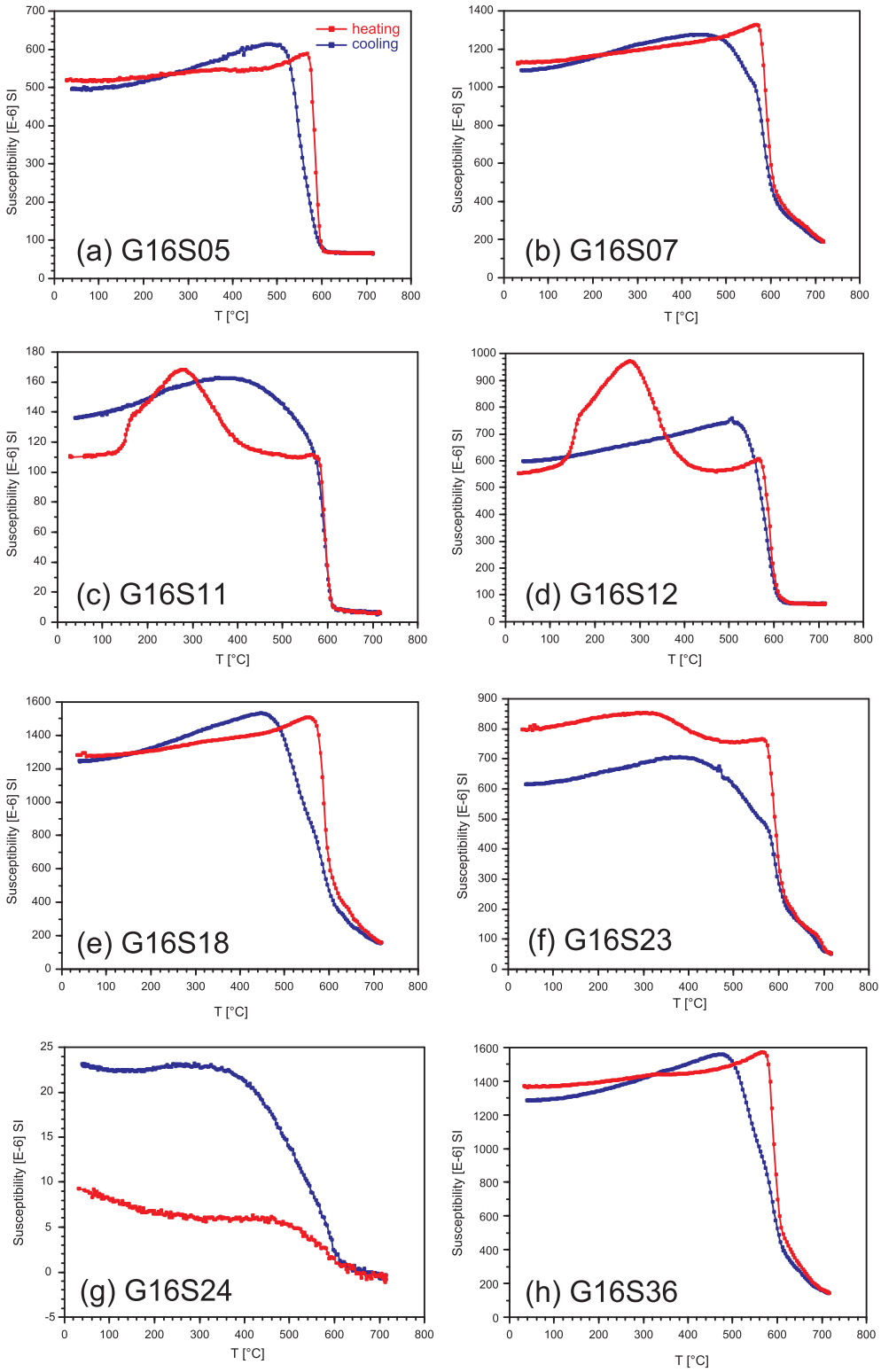

Fig. 7. Results of thermomagnetic susceptibility analysis. Heating and cooling curves are represented by red and blue colors, respectively. (For interpretation of the references to colour in this figure legend, the reader is referred to the web version of this article.)

approaching the unblocking temperature or coercivity of magnetite, so it is hard to isolate a decay-to-origin component. However, the directions move towards the NW-up BDD-reference direction (Group An; Fig. 10). The pattern of vector-endpoint diagrams clearly shows a partial remagnetization. Based on the aeromagnetic anomaly map and geochronology, it is likely that sites G16S16 and G16S37 (947 ± 4 Ma)

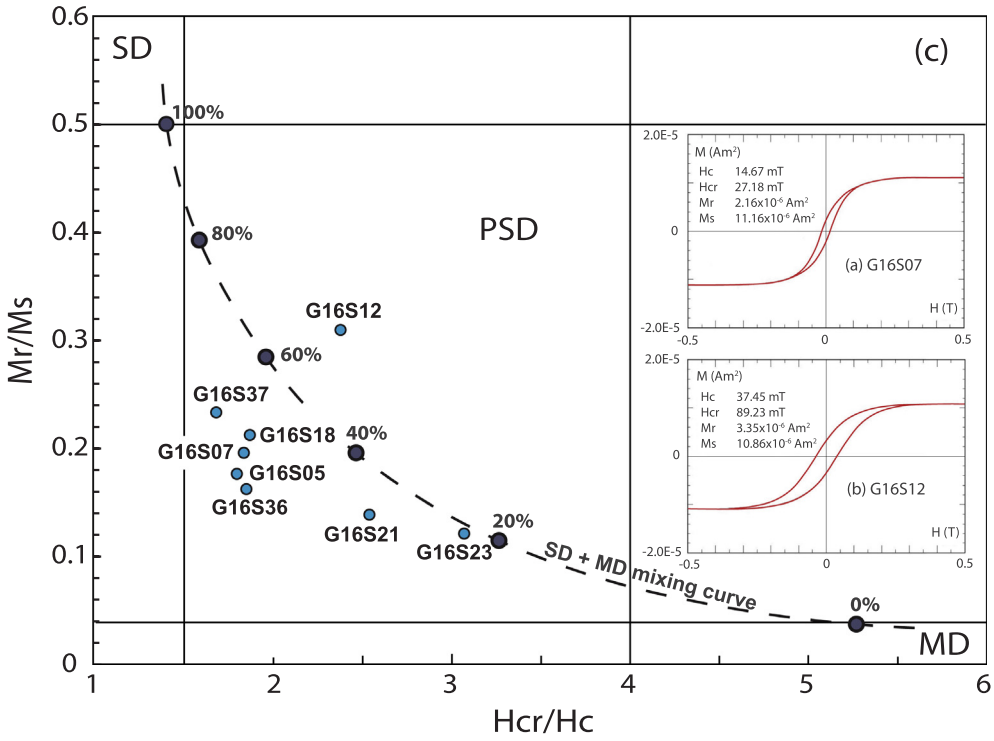

Fig. 8. Hysteresis ratios of BDD dykes displayed in the Day plot (Day et al., 1977). The dashed line shows the SD/MD theoretical mixing curve (Dunlop, 2002). Inset plots are representative hysteresis loops after the correction of paramagnetic slope.

are from a southeastward extension of the Nornäs dyke, and they also give identical paleomagnetic results and similar ages. Therefore, we interpret that the Nornäs dyke consists of some PSD grains that carry a PDF overprint, difficult to be adequately removed due to the strong overlap of unblocking temperature or coercivity with SD magnetite grains. Since a clear decay-to-origin component cannot be isolated from sites G16S05, G16S06, G16S16 and G16S37, we tried to use great circle method for paleomagnetic analyses. Combining all great circles from these four sites of the Nornäs dyke, we obtained a mean direction of Declination = 307.9°, Inclination = −35.3°, α_{95} = 2.9°, which we named it as "Nornäs new", the direction of which is very close to the NW-up BDD-reference direction (Group An; Fig. 10; Table 2). The Nornäs new direction is likely the primary remanence of the Nornäs dyke. However, without any sample bearing a clear decay-to-origin component, we prefer to exclude this Nornäs new mean direction from the paleomagnetic statistics of this study. The steep ChRM direction of previous work was calculated from the minimum scatter in magnetic directions after demagnetization in AF intensities of 10–20 mT (Piper and Smith, 1980; Bylund, 1985; Table 2), which is too low to remove the PDF overprint. Another dyke, G16S14, yields similar demagnetization pattern as the Nornäs dyke and is also likely affected by partial remagnetization in the PDF direction.

5. Discussion

5.1. Origin of BDD dykes – A giant circumferential swarm?

Arcuate-shaped swarms have been increasingly reported in different geological settings with various intrusion ages (Denyszyn et al., 2009; Mäkitie et al., 2014; Buchan and Ernst, 2018). However, the physical mechanism explaining the unusual geometry is still under debate. Interestingly, the coronae on Venus are also characterized by similar ring-shaped surface expressions and are thought to be associated with tectono-magmatic processes (Squyres et al., 1992). Are the arcuate-shaped swarms on Earth and Venusian coronae intrinsically related in terms of their origin?

Venusian coronae have two components: a radiating system and a circumferential system, both of which are presumably underlain by dykes (Ernst et al., 2003). In order to explain their distinctive tectonic and topographic features, Stofan and Head (1990) suggested a mantle plume origin for coronae. The radiating system is argued to be related to the upwelling of hot magma, causing surface uplift and dyke intrusion, while the circumferential system is due to gravitational collapse as the mantle upwelling ceases. If this mechanism is true, it is expected that the radiating system would predate the circumferential system.

Ernst and Buchan (1998) first proposed that the arcuate-shaped swarms on the Earth could be analogous to Venusian coronae. They defined any arcuate-shaped swarm as a giant circumferential swarm if it has a primary circular or elliptical geometry with an arc of > 45° and a diameter > 60 km (Buchan and Ernst, 2016). Based on these criteria, BDD dykes would be classified as a giant circumferential swarm, accounting for their 750-km long, ~60° arcuate geometry. The primary curved geometry is supported by tectonic coherence of southern Sweden since Neoproterozoic time, and also the demonstrably high-quality BDD paleomagnetic data, which discern no structural rotation following emplacement. Therefore, the critical test of this hypothesis hinges on another two aspects. Is there a corresponding radiating system? And if so, is the radiating system older than BDD dykes, as required by Stofan and Head (1990)'s model?

The available ages of BDD dykes/sills suggest prolonged intrusions

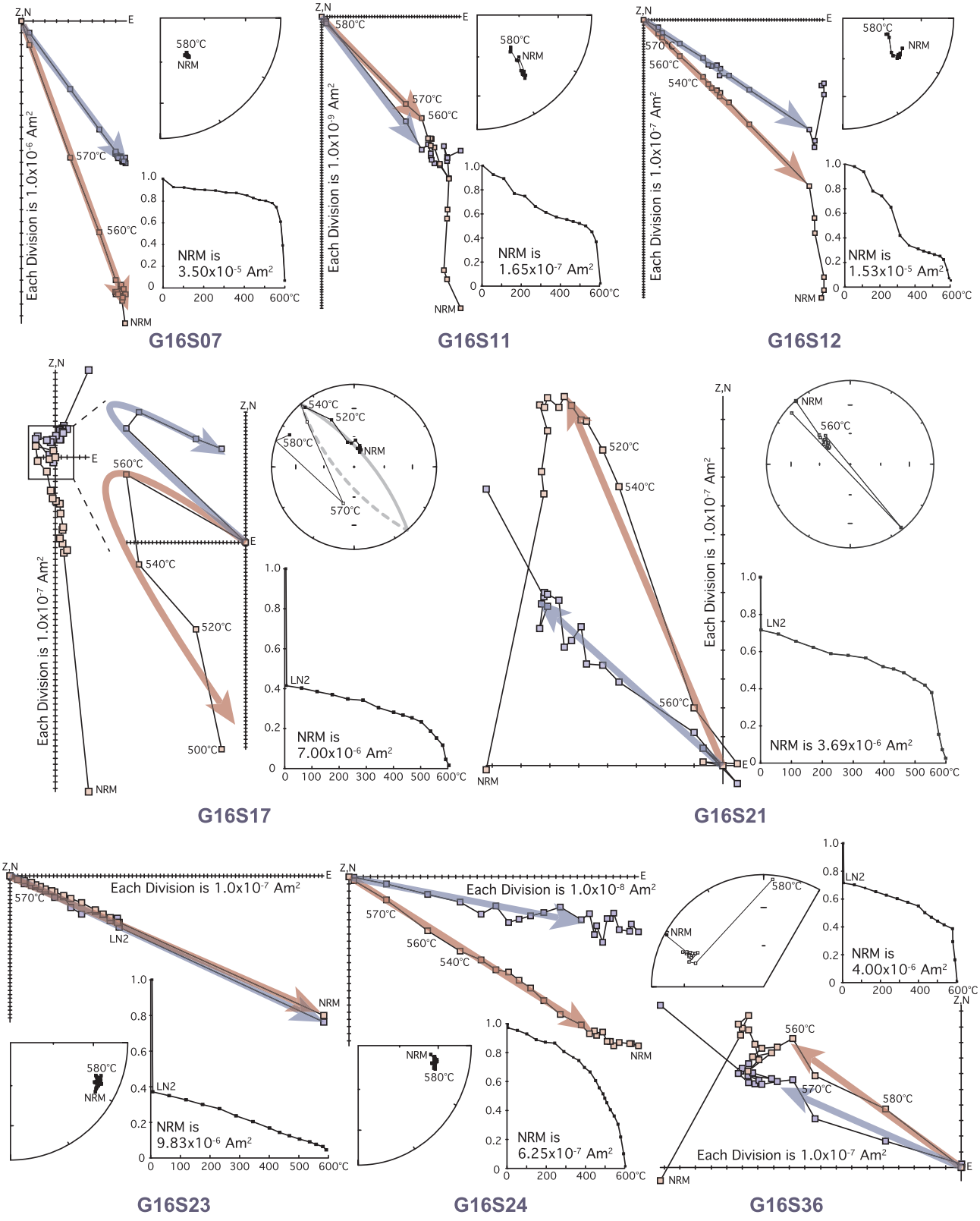

Fig. 9. Representative thermal demagnetization results of BDD dykes. Vector-endpoint diagrams are shown (Zijderveld, 1967), with equal-area stereonet plots and remanence intensity (J/J_0) plots. ChRMs are plotted with blue and red arrows representing declinations and inclinations, respectively. (For interpretation of the references to colour in this figure legend, the reader is referred to the web version of this article.)

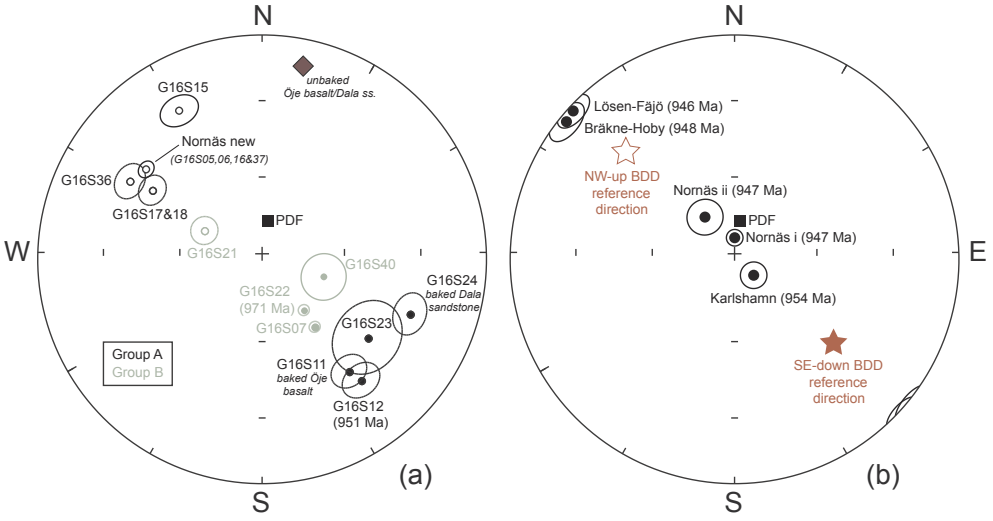

Fig. 10. (a) Equal-area stereonet projection summarizing the ChRMs of BDD dykes with corresponding 95% confidence cones. Unbaked paleomagnetic direction of Öje basalt and Dala sandstone is suggested by the purple diamond. Present-day field direction of sampling area is indicated by the black square. Closed and open circles show the downwards and upwards paleomagnetic inclinations. PDF = present-day field. (b) Equal-area stereonet projection of anomalous BDD dyke directions. Red stars indicate the BDD reference directions. (For interpretation of the references to colour in this figure legend, the reader is referred to the web version of this article.)

(Fig. 5). Given the distribution of these ages, there seems to be 3 possible pulses of BDD intrusions, first pulse from 980 Ma to 965 Ma; second from 955 Ma to 945 Ma; third from 942 Ma to 935 Ma (Fig. 5), although definitive conclusion still needs more geochronological studies. Any radiating-system candidate should be older or at least very close to the first pulse of BDD intrusions. The Göteborg-Slussen dykes in southwestern Sweden were proposed as the radiating system linked to the purported mantle plume, because their trends are sub-orthogonal to those of the BDD dykes (Fig. 2; Buchan and Ernst, 2016). However, the Tuve dyke, which belongs to the Göteborg-Slussen dyke suite, is dated to be 935 ± 3 Ma by the U-Pb baddeleyite method (Hellström et al., 2004), which approaches equivalency to the youngest members of BDD dykes but is tens of millions of years younger than the majority of BDD dykes. Another candidate for the radiating system might be the Hunnedalen dykes in western Norway (Fig. 2), trending NE-SW, sub-orthogonal to BDD dykes. But the Hunnedalen dykes are ~100 million years younger than BDD dykes (Walderhaug et al., 1999), excluding their possibility of being the radiating component. In general, geochronological data do not support Buchan and Ernst (2016)'s mantle plume model. The prolonged intrusion interval of BDD dykes is more likely connected with the plate boundary forces causing gravitational extension in the Baltic foreland during protracted waning stages of the Sveconorwegian orogeny. Variable orientation of the regional stress field might be the cause for the primary arcuate geometry (Wahlgren et al., 1994).

5.2. Implications for paleogeography of Baltica

Large variances have been observed in the paleomagnetic results of BDD dykes (Fig. 10b; Table 2), which have been interpreted differently in previous studies (e.g., Pesonen and Klein, 2013). Here, we summarize available paleomagnetic and geochronological data of BDD dykes in the literature (Fig. 5; Table 2), in an attempt to examine each proposed model, and then discuss their implications. First, if we assume that all BDD results are reliable without any remagnetization/contamination, the variances in BDD dyke remanences would be substantial (Table 2), for instance, the very steep inclinations of 947 Ma Nornäs dyke and 954 Ma Karlshamn dyke, and the very shallow inclinations of 946 Ma Fäjö dyke and 948 Ma Bräkne-Hoby dyke (Fig. 10b). These variances, occurring within a fairly short time interval (less than 10 Ma), if interpreted as plate motion, would require unrealistically fast drift rates of Baltica, contradicting geologically younger plate tectonic speeds. Even true polar wander, which might occur as fast as ~ 6° per Myr (Rose and Buffett, 2017), is insufficient to reconcile the variances in BDD remanences. Another possibility might be a non-GAD field, but even then, the entire BDD dataset would be difficult to explain unless departures from GAD were extreme. For example, Pesonen et al. (2012) show that with 11% octupole field (relative to a dominant GAD field), the inclination shallowing effect will approach a maximum ~10° at mid-paleolatitudes. However, the inclination differences among BDD remanences are mostly larger than 10°, and some even reach 70–80° (Table 2). Only if the transient ancient magnetic field was totally dominated by the octupole component (Tauxe, 2005) or by an ephemeral equatorial dipole field (Abrajevitch and Van der Voo, 2010) can the large inclination differences be explained.

After the experience gained from careful demagnetization procedures in our study, we are suspicious that the large variances of remanence in the entire BDD dataset likely result from selective remagnetization. The 947 Ma Nornäs dyke, after being subjected to detailed demagnetization, shows that the remanence gradually moves away from the previously determined ChRM and towards the NW-up BDD-reference direction (Figs. 10 and 11). In fact, based on the great circle analyses, the primary remanence of the Nornäs dyke should be the same as that of Group An, and the low-temperature or low-AF remanence component of the Nornäs dyke is NNW and steep down, very close to the PDF direction. Hence, it is very likely that the Nornäs dyke was affected by partial remagnetization and component mixing due to overlapping coercivity and/or unblocking temperature spectra. That concept impels us to doubt the robustness of other anomalous directions, especially the 954 Ma Karlshamn dyke, for which the published ChRM direction is very close to the PDF direction (Fig. 10b). Also, as the remanences of 946 Ma Lösen-Fäjö and 948 Ma Bräkne-Hoby dykes are half-way between the PDF direction and the NW-up BDD-reference direction (Group An), they could possibly carry substantial PDF overprints as well. Besides, the previously published directions of the Nornäs, Lösen-Fäjö, Karlshamn and Bräkne-Hoby dykes were calculated using the minimum scatter of data at 10 mT, 20 mT, 30 mT or 40 mT (Patchett and Bylund, 1977; Piper and Smith, 1980; Bylund, 1985; Table 2). AF demagnetization below 30 mT is generally too low to be

Table 2
Summary of paleomagnetic results of BDD dykes.

Dyke	Slat (°N)	Slon (°E)	Age (Ma)	Dec (°)	Inc (°)	α_{95} (°)	N/n	Plat (°N)	Plon (°E)	A_{95} (°)	Group	Reference	Comment
G16S22	61.6043	13.2260	971 ± 7	140.6	66.1	2.0	1/10	−24.5	220.8	3.0	Br	This study	NW-SE trending (324°)
G16S21	61.5937	13.0047		296.5	−66.5	5.0	1/8	–32.1	236.3	7.5	Bn	This study	NW-SE trending
Nornäs ii	61.42	13.21	946.8 ± 1.2	325.0	71.3	6.5	1/4	71.0	282.0	10.5	–	Bylund (1985); Söderlund et al. (2005)	remanance at 10 mT[a]
Nornäs i	61.42	13.21	946.8 ± 1.2	0.4	82.2	3.0	1/6	77.0	14.0	6.0	–	Piper and Smith (1980); Söderlund et al. (2005)	–
G16S05	61.4230	13.2150		Nornäs dyke, partial remagnetization and vector component contamination							–	This study	NW-SE trending (315°)
G16S06	61.4207	13.2202		Nornäs dyke, partial remagnetization and vector component contamination							–	This study	NW-SE trending (315°)
G16S07	61.2557	13.7790		142.1	58.7	2.0	1/9	−15.3	223.2	2.6	Br	This study	NW-SE trending (330°)
G16S17	61.2504	13.4103		305.5	−45.5	4.2	1/4	−8.5	240.6	4.3	–	This study	NW-SE trending (315°), same dyke as G16S18
G16S18	61.2464	13.4186		300.5	−39.8	9.4	1/5	−6.4	246.6	8.7	–	This study	NW-SE trending (315°), same dyke as G16S17
G16S17&18 comb.	–	–		302.2	−41.7	5.2	1/9	−7.0	244.6	5.0	An	This study	–
G16S24	61.1999	13.1505	~1460	110.3	30.4	6.8	1/8	−5.0	257.8	5.6	–	This study	baked Dala sandstone
G16S23	61.1992	13.1515		126.6	40.9	12.9	1/7	−4.9	240.8	12.2	Ar	This study	NW-SE trending (320°)
G16S14	61.1455	12.7273		demagnetization behavior like the Nornäs dyke, partial remagnetization and vector component contamination							–	This study	NW-SE trending
G16S16	61.1118	13.8530		southern extension of the Nornäs dyke, partial remagnetization and vector component contamination							–	This study	NW-SE trending (325°), width ~8 m
G16S15	61.0949	13.0151		330.7	−24.7	6.2	1/3	12.4	222.1	4.7	An	This study	NW-SE trending (325°)
G16S09	60.9265	13.1784		inconsistent directions within dyke							–	This study	NW-SE trending (305°), same dyke as G16S10
G16S37	60.9181	14.1043	947 ± 4	southern extension of the Nornäs dyke, partial remagnetization and vector component contamination							–	This study	NW-SE trending (325°)
Nornäs new (G16S05,06,16& 37 comb.)	–	–		307.9	−35.3	2.9	4/22	−0.8	241.7	2.6	–	This study	Mean direction calculated using great circle method
G16S10	60.8878	13.3006		inconsistent directions within dyke							–	This study	NW-SE trending (305°), same dyke as G16S09
G16S36	60.8284	14.2725		300.6	–32.0	5.9	1/8	−1.4	249.5	5.0	An	This study	NW-SE trending
G16S11	60.8077	13.5783	~1460	140.7	30.9	6.5	1/9	−14.9	223.0	2.6	–	This study	baked Öje basalt
G16S12	60.8077	13.5783	951 ± 5	142.2	36.9	6.2	1/9	3.1	228.7	5.6	Ar	This study	NW-SE trending (324°)
Andersbo	60.76	15.41		143.0	42.0	9.0	1/7	1.0	229.0	7.3	–	Bylund and Elming (1992)	–
G16S13	60.7147	13.3904		153.2	8.3	7.3	1/8	21.8	222.4	5.2	–	This study	NW-SE trending
Ejen	60.67	14.79		128.0	24.0	9.0	1/8	6.0	245.8	6.6	–	Bylund (1985)	remanance at 20 mT[a]
Falun (new)	60.59	15.58	945.7 ± 1.2	128.7	37.9	3.0	1/9	−1.7	242.3	2.6	Ar	Elming et al. (2014); Söderlund et al. (2005)	NW-SE trending (330°)
Falun (old)	60.59	15.58	945.7 ± 1.2	131.4	45.8	5.6	1/10	−6.1	237.6	5.7	–	Patchett and Bylund (1977); Söderlund et al. (2005)	remanance at 20 mT[a]
Gällsjön	60.51	14.53		136.0	48.0	12.0	1/5	18.0	241.0	8.5	–	Bylund and Elming (1992)	–
G16S40	60.3185	14.2210		106.0	67.0	8.3	1/9	−35.0	243.7	12.5	Br	This study	NW-SE trending (330°)
G16S39	60.3024	13.8662		inconsistent directions within dyke							–	This study	NW-SE trending, same dyke as G16S38
G16S38	60.3016	13.8672		inconsistent directions within dyke							–	This study	NW-SE trending, same dyke as G16S39
Årby	59.27	16.46		142.5	52.4	7.0	1/6	−7.3	227.4	8.0	–	Patchett and Bylund (1977)	remanance at 20 mT[a]
Marbystrand	58.61	16.48		127.5	31.1	3.6	1/9	3.3	246.0	3.0	–	Elming et al. (2014)	NW-SE trending (310°)
Y1	58.58	16.33	938 ± 4	311.2	−43.3	5.7	1/13	−3.4	239.0	4.0	An	Elming et al. (2014)	NE-SE trending (40°)
Y2	58.58	16.33	941 ± 6	313.3	−40.7	7.4	1/14	−0.5	238.3	7.0	An	Elming et al. (2014)	NE-SE trending (40°)
Slussen	58.2	12.2		300.9	−26.5	11.5	1/6	3.2	248.5	9.2	An	Pisarevsky and Bylund (2006)	–
Tuve	57.8	11.8	935 ± 3	122.2	53.7	3.2	2/23	−14.0	237.9	3.7	Ar	Pisarevsky and Bylund (2006); Hellström et al. (2004)	–
Small	57.8	11.8		124.5	54.6	7.4	1/3	−13.9	235.8	8.8	Ar	Pisarevsky and Bylund (2006)	–
Hjuvik	57.7	11.7		118.8	37.1	11.5	1/12	−3.3	246.9	10.3	Ar	Pisarevsky and Bylund (2006)	–

(*continued on next page*)

Table 2 (*continued*)

Dyke	Slat (°N)	Slon (°E)	Age (Ma)	Dec (°)	Inc (°)	α_{95} (°)	N/n	Plat (°N)	Plon (°E)	A_{95} (°)	Group	Reference	Comment
Sjunnaryd (sill)	57.7	14.8		317.1	−28.9	15.1	1/4	8.8	236.4	12.4	–	Pesonen and Klein (2013)	–
Nilstorp (sill)	57.64	14.83	966 ± 5	315.2	−27.4	9.7	1/6	9.0	238.5	7.8	–	Patchett and Bylund (1977); Söderlund et al. (2005)	remanance at 40 mT[a]
Tärnö	56.27	15.06		312.8	−41.9	4.8	1/5	0.3	237.0	4.6	–	Patchett and Bylund (1977)	remanance at 30 mT[a]
Bräkne-Hoby	56.26	15.18	948.1 ± 1.4	309.3	3.6	6.1	1/7	22.2	251.9	4.3	–	Patchett and Bylund (1977); Söderlund et al. (2005)	remanance at 40 mT[a]
Lösen-Fäjö	56.17	15.69	945.8 ± 1.0	312.6	2.6	5.4	1/6	23.3	248.9	3.8	–	Patchett and Bylund (1977); Söderlund et al. (2005)	remanance at 20 mT[a]
Väby	56.17	15.22		137.0	33.0	10.0	1/3	8.0	236.0	8.4	–	Poorter (1975)	remanance at 10 mT[a]
Karlshamn	56.15	14.86	954.2 ± 1.1	129.0	81.0	4.8	1/9	−43.2	213.5	9.1	–	Patchett and Bylund (1977); Söderlund et al. (2004a)	remanance at 30 mT[a]
Group A Mean	–	–		**127.6**	**65.4**	**9.7**	**12/116**	**−2.6**	**239.6**	**5.8**	–		**Averaging 12 dykes in Group An/Ar listed in this table**
Group B Mean	–	–		**128.8**	**39.6**	**6.5**	**4/36**	**−27.0**	**230.4**	**14.9**	–		**Averaging 4 dykes in Group Bn/Br listed in this table**

Note: Slat/Slon = site geographic latitide/longitude, Dec = declination, Inc = inclination, Plat/Plon = paleomagnetic pole latitude/longitude, N/n = number of site/sample, α_{95} = radius of 95% confidence cone of the mean direction, A_{95} = radius of 95% confidence cone of the paleomagnetic pole.

[a] Least scatter of data at alternating-field step used for mean vector calculation.

pertinent to Precambrian paleomagnetic remanence preservation. If two components have strongly overlapping demagnetization spectra, higher AF intensities do not necessarily guarantee a successful removal of a partial overprint. With more sophisticated laboratory equipment and more accurate analytical methods (principal component analysis, great circle method etc.) now available, we suggest a re-study of these dykes before using their directions for geophysical interpretations.

Because we suspect the reliability of some results of BDD dykes in previous studies, either due to the inadequate demagnetization (e.g., low AF field) or outdated analytical methods (e.g., least scatter method for averaging paleomagnetic directions), for subsequent discussion we only focus on the results that we can be assured to lack an overprint/contamination. This would yield 12 dykes in Group A (6 dykes in Group An and 6 dykes in Group Ar; Table 2) and 4 dykes in Group B (1 dyke in Group Bn and 3 dykes in Group Br; Table 2). We admit that by this treatment the paleomagnetic dataset of BDD dykes is reduced, but we can test for averaging out the paleosecular variation (PSV) by calculating the angular dispersion (S) for each of the two poles we obtained from Groups A and B, respectively, following the approximation equation:

$$S = \frac{81^\circ}{\sqrt{k}}$$

where k is the best estimate of precision parameter (Butler, 1992).

The calculated S values are plotted against the 1.5–0.5 Ga model G curve fitted by Veikkolainen and Pesonen (2014). It is noted that the 951–935 Ma pole obtained from Group A matches the model G curve very well (Fig. 12; Table 3), which means that even though we used a smaller dataset, the number of dykes seems sufficient to average out the PSV. In contrast, the 971 Ma pole obtained from Group B falls below the model G curve (Fig. 12; Table 3). Since there are only 4 dykes in Group B, this pole is considered merely as a VGP, and more dykes in this group are needed to provide a paleomagnetic pole in future studies. Further geochronology on Group B dykes would also be useful to assess whether they are restricted to a narrow age range.

The early Neoproterozoic apparent polar wander (APW) path of Baltica, known as the Sveconorwegian loop, is under debate in terms of its shape and form. Previously, the Sveconorwegian loop (as shown in the South Pacific) was generally assumed to exhibit counterclockwise motion (Fig. 13a; Elming et al., 1993). However, some have suggested that the southernmost part of the Sveconorwegian loop represents a post-900 Ma delayed remanence acquisition during slow exhumation of the deep-seated igneous rocks (Walderhaug et al., 1999; Brown and McEnroe, 2004). Pisarevsky and Bylund (2006) speculated that the delayed acquisition is probably caused by low-temperature chemical alteration. Elming et al. (2014) proposed a clockwise motion of the south-Pacific polarity representation of the Sveconorwegian loop, incorporating the 946–935 Ma equatorial pole and assuming that the southernmost part of the loop is post-900 Ma (Fig. 13a). Similarly, the early Neoproterozoic APW path of Laurentia (also viewed in the south-Pacific polarity representation) is also interpreted as either clockwise (Hyodo and Dunlop, 1993) or counterclockwise (Weil et al., 2006). Regardless of uncertainties in the APW paths of two cratons, geological evidence supports a proximity of Baltica and Laurentia during the Neoproterozoic time (Cawood and Pisarevsky, 2006).

Our results from BDD dykes support the equatorial pole for Baltica at 951–935 Ma, similar to the result of Elming et al. (2014). In addition, we obtained a 971 Ma VGP for Baltica, suggesting a high-paleolatitude position. Brown and McEnroe (2012) studied paleomagnetism of the igneous and metamorphic rocks in the Adirondack Highlands of Laurentia. Performing careful rock-magnetic and petrological studies, they generated several poles with modeled cooling ages of 990–960 Ma. We also performed the PSV test of the 970 Ma and 960 Ma poles from Brown and McEnroe (2012), which suggests that the PSV has been averaged out from these two poles (Fig. 12; Table 3). Cratonic reconstruction using these poles and our new 971 Ma VGP permits a close

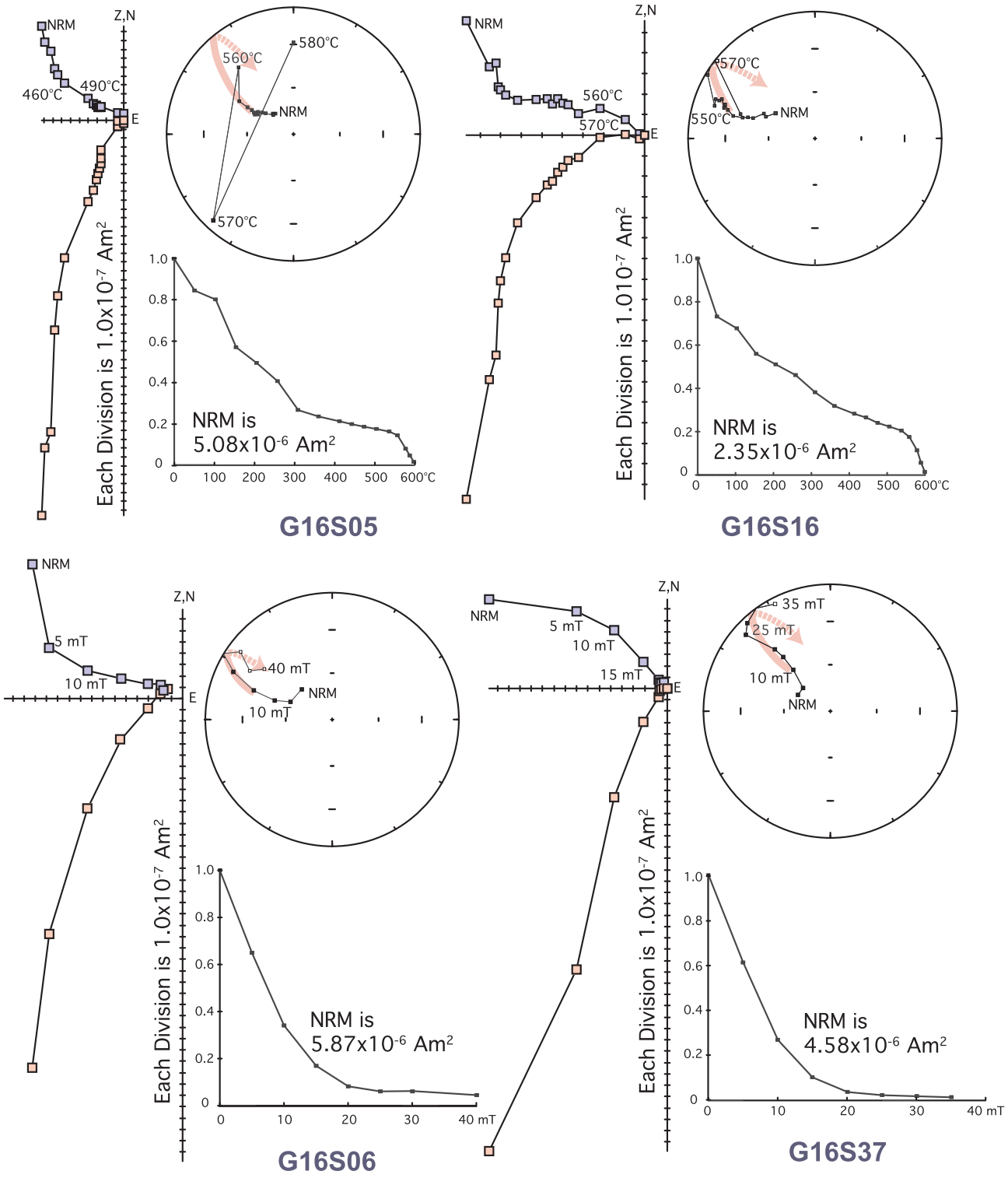

Fig. 11. Typical thermal and alternating-field demagnetization behaviors of the Nornäs dyke. Vector-endpoint diagrams (Zijderveld, 1967), equal-area stereonet plots and remanence intensity (J/J_0) plots are shown. Red solid/dashed lines indicate the trending of remanent directions in lower/upper hemisphere. (For interpretation of the references to colour in this figure legend, the reader is referred to the web version of this article.)

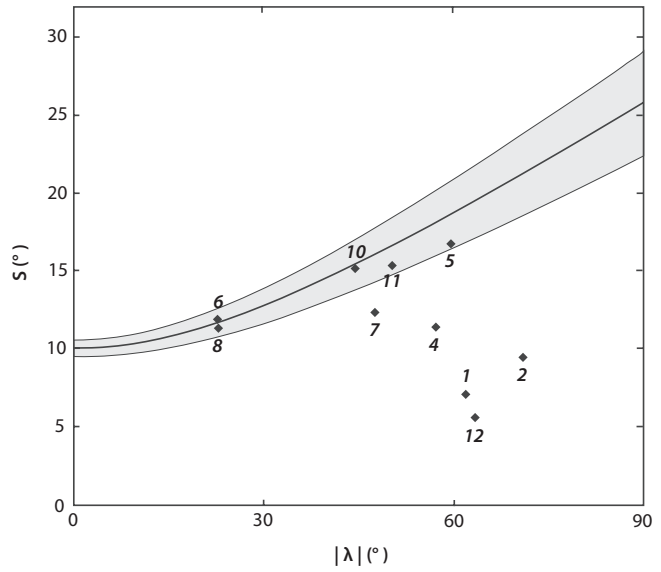

Fig. 12. Paleosecular variation (PSV) test. The thick black line is the 1.5–0.5 Ga model G curve from Veikkolainen and Pesonen (2014). The gray area is the corresponding error limits (2σ). Numbers are paleomagnetic poles used in the paleogeographic reconstruction, which are listed in Table 3.

position between Baltica and Laurentia at 970–960 Ma. The reconstructed positions of two cratons allow the Sveconorwegian and Grenville orogenies to be a continuous belt, which has been suggested in many other studies (e.g., Li et al., 2008; although see Gower et al., 2008, for cautionary details). The Sveconorwegian and Grenville loops seem to have some oscillatory components (Fig. 13), which could be attributed to plate motions or true polar wander (Evans, 2009). In this scenario, the paleogeographic evolution of the two cratons is characterized by high- to low-latitude drift between 970–960 Ma and 950–935 Ma, and a return from low- to high-latitude by 920–870 Ma (Fig. 14). Notably, all three pole groups include at least one result that appears to average PSV adequately (Fig. 12). The implied drifting speed is of ~100–150 km/Ma, which is fast but is a reasonable rate for either plate tectonics or true polar wander. Deconvolving those two processes will require more detailed paleomagnetic work from Baltica, Laurentia, and other cratons with suitably complete early Neoproterozoic geological records.

6. Conclusions

We present a detailed paleomagnetic, rock magnetic and anisotropy of magnetic susceptibility, and geochronological study of the Blekinge-Dalarna dolerite dykes, which leads to following conclusions:

(1) Positive baked-contact, reversal and PSV tests support the reliability of the equatorial paleomagnetic pole for Baltica at 951–935 Ma (Plat = −2.6°N, Plon = 239.6°E, A_{95} = 5.8°, N = 12 dykes), which can be used as a key pole to constrain the paleogeography of Baltica.
(2) The anomalous paleomagnetic direction obtained from the 947 Ma Nornäs dyke is probably due to a PDF overprint that was not adequately removed by low alternating-field demagnetization levels in previous studies, instead of originating from true polar wander, or abnormal geomagnetic field behavior. PDF component contamination is suspected in other anomalously-directed BDD dykes.
(3) A well-dated 971 Ma VGP (Plat = −27.0°N, Plon = 230.4°E, A_{95} = 14.9°) from four BDD dykes, in concert with same-age poles from Laurentia, suggests a high-latitude position for Baltica in proto-Rodinia. Paleogeographic reconstruction demonstrates that

Table 3
Paleomagnetic poles constrain the early Neoproterozoic paleogeographic reconstruction of Baltica and Laurentia.

#	Paleomagnetic Pole	Dec (°)	Inc (°)	α_{95} (°)	k	N/n	Plat (°N)	Plon (°E)	A_{95} (°)	S (°)	|λ| (°)	Age (Ma)	1	2	3	4	5	6	7	Q	Reference
Baltica																					
1	Humnedalen dykes	294.0	−75.0	6.0	115	6/69	−41.0	222.0	10.5	7.2	61.8	848 ± 27[a]; 855 ± 59[b]	1	1	1	0	1	0	1	5	Walderhaug et al. (1999)
2	Egersund-Ogna anorthosite	325.9	−80.1	4.9	73	13/69	−42.1	200.4	9.0	9.5	70.8	900[c]	1	1	1	0	0	0	1	4	Brown and McEnroe (2004)
3	Egersund anorthosite	–	–	–	–	76/–	−43.5	213.7	3.6	–	–	900[c]	0	1	1	0	0	0	1	3	Stearn and Piper (1984); Walderhaug et al. (1999)
4	Rogaland Igneous Complex	269.0	−72.0	11.0	49	5/24	−45.9	238.4	18.2	11.5	57.0	869 ± 14[a]	1	0	1	1	0	0	1	4	Walderhaug et al. (2007)
5	Bjerkreim-Sokndal intrusion	303.4	−73.5	3.7	24	66/354	−35.9	217.9	6.0	16.8	59.4	916[c]	1	1	1	0	1	0	1	5	Brown and McEnroe (2015)
6	Mean 951–935 Ma Baltica pole	308.8	−39.6	6.5	42	12/116	−2.6	239.6	5.8	12.0	22.5	951 – 935[d]	1	1	1	1	1	1	1	7	This study
7	971 Ma BDD dykes VGP	307.6	−65.4	14.2	68	4/36	−27.0	230.4	14.9	12.4	47.5	971 ± 7[d]	1	0	1	0	1	1	1	5	This study
8	Laanila-Ristijärvi dykes	355.5	−40.0	17.5	51	3/7	−2.1	212.2	16.4	11.4	22.8	1042 ± 50[b]	0	0	1	1	1	0	0	3	Mertanen et al. (1996)
9	Bamble Intrusion mean	–	–	–	–	–	3.0	217.0	15.0	–	–	1100–1040	0	1	1	0	0	0	0	2	Meert and Torsvik (2003)
Laurentia																					
10	Adirondack microcline gneisses	289.2	−62.8	7.6	29	14/80	−18.4	151.1	10.5	15.2	44.2	960[c]	1	1	1	0	0	1	1	5	Brown and McEnroe (2012)
11	Adirondack metamorphic anorthosites and other rocks	283.9	−67.3	7.7	28	14/68	−25.1	149.0	11.6	15.4	50.1	970[c]	1	1	1	0	0	1	1	5	Brown and McEnroe (2012)
12	Adirondack fayalite granites	297.0	−75.8	3.9	199	8/40	−28.4	132.7	6.9	5.7	63.2	990[c]	1	1	1	0	0	1	1	5	Brown and McEnroe (2012)

Note: Dec = declination, Inc = inclination, α_{95} = radius of 95% confidence cone of the mean direction, k = precision parameter, N/n = number of site/sample, Plat/Plon = paleomagnetic pole latitude/longitude, A_{95} = radius of 95% confidence cone of the paleomagnetic pole, S = angular dispersion of VGPs, |λ| = absolute value of paleolatitude, Q = sum of quality criteria (Van der Voo, 1990).

[a] Ar-Ar biotite ages.
[b] Sm-Nd whole-rock ages.
[c] Cooling ages.
[d] U-Pb baddeleyite ages.

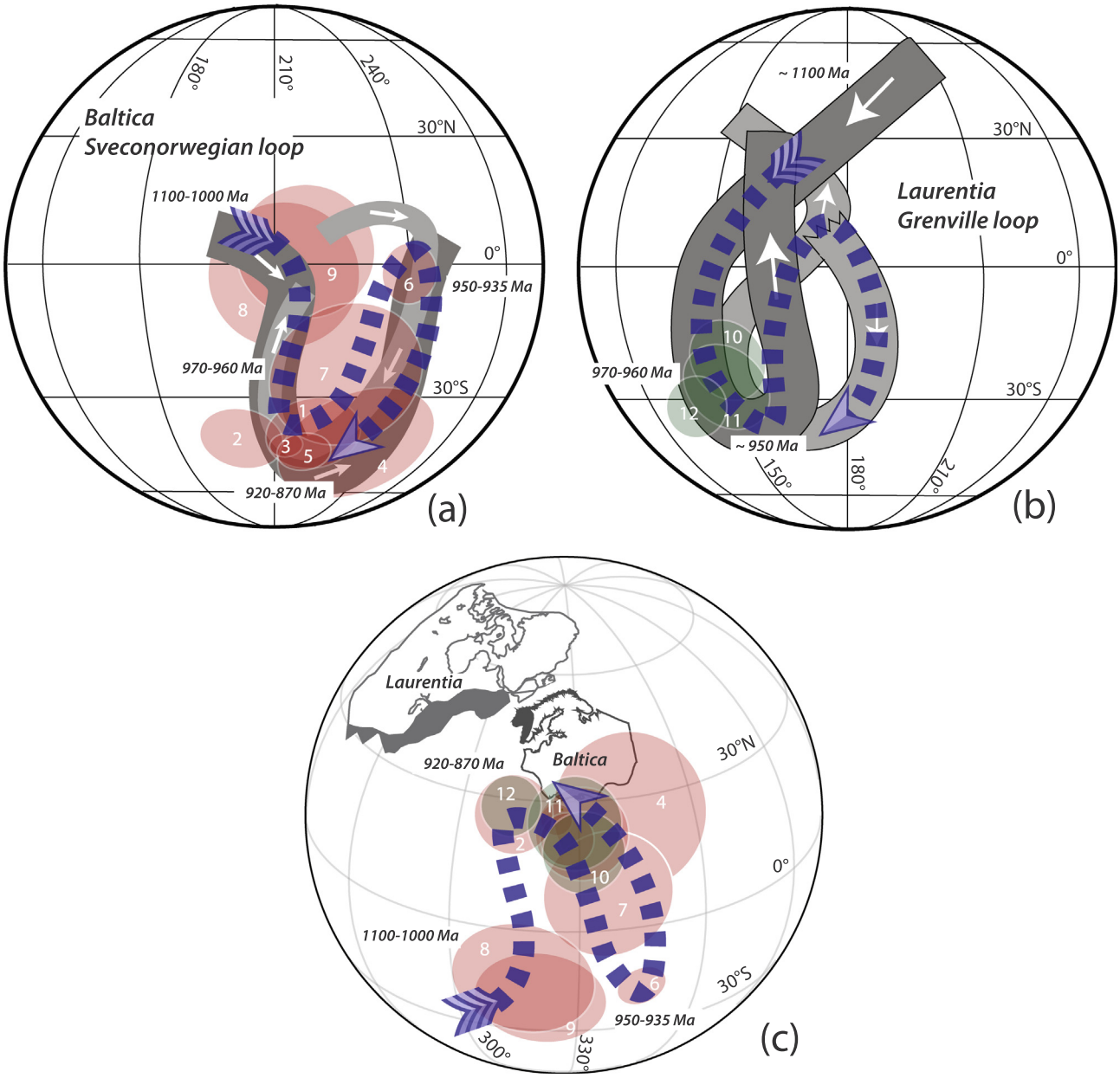

Fig. 13. (a) Sveconorwegian loop for Baltica. Counterclockwise motion is from Elming et al. (1993) and clockwise motion is from Elming et al. (2014). (b) Grenville loop for Laurentia. Counterclockwise motion is from Weil et al. (1998) and clockwise motion is from Hyodo and Dunlop (1993). (c) Coeval 1000–850 Ma paleomagnetic poles from Baltica and Laurentia in present North America reference frame. White arrows indicate the younging directions of apparent polar wander paths. Blue dash lines indicate new loop proposed by this study. Red poles are from Baltica and green poles are from Laurentia. Poles' numbers are listed in Table 3. (For interpretation of the references to colour in this figure legend, the reader is referred to the web version of this article.)

Baltica and Laurentia drifted together towards low latitude between 970–960 Ma and 950–935 Ma, and moved back to high latitude by 920–870 Ma. In this scenario, the apparent polar wander paths of Baltica and Laurentia would be more complicated than either the Sveconorwegian or the Grenville loops considered in isolation.

(4) Based on published ages of BDD dykes and adjacent sub-orthogonal dykes, it seems that the requirement of a single mantle plume model is not satisfied. The BDD dykes more likely result from plate boundary forces associated with the Sveconorwegian orogeny. The arcuate geometry could be associated with a spatially varying regional stress distribution.

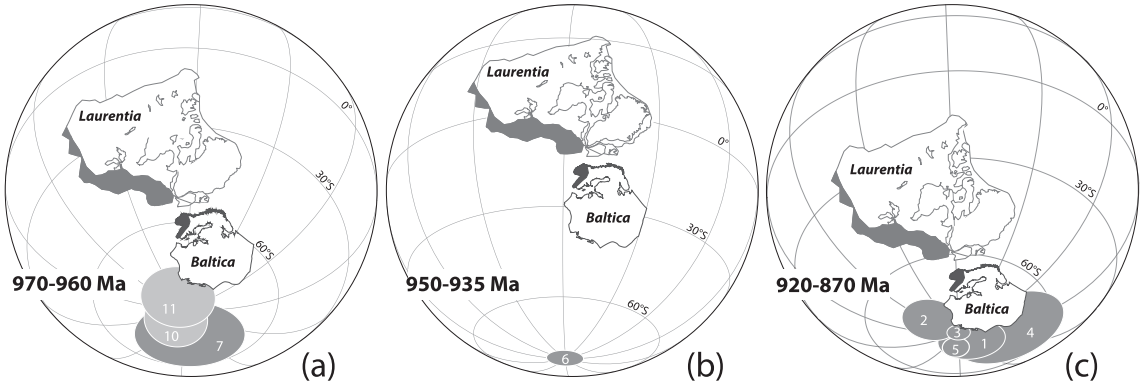

Fig. 14. Paleogeographic reconstructions of Baltica and Laurentia. (a) 970–960 Ma (Euler pole of Laurentia to absolute reference: 22.4°N, 100.6°E, 127.6°; Euler pole of Baltica to Laurentia: 75.8°N, 95.7°E, −59.2°); (b) 950–935 Ma (Euler pole of Laurentia to absolute reference: −37.9°N, −65.5°E, −99.8°; Euler pole of Baltica to Laurentia: 75.8°N, 95.7°E, −59.2°); (c) 920–870 Ma (Euler pole of Laurentia to absolute reference: −15.6°N, −93.5°E, −125.9°; Euler pole of Baltica to Laurentia: 75.8°N, 95.7°E, −59.2°). Paleomagnetic poles used for reconstruction are listed and numbered in Table 3. Dark and light gray poles are from Baltica and Laurentia, respectively.

Acknowledgements

We would like to thank Anna Sartell at Lund University for preparing baddeleyite grains for U-Pb dating, and Stephen Victor for helping with hysteresis loop measurement in Yale Archaeomagnetism Laboratory. Thanks are also due to Magnus Ripa at the Geological Survey of Sweden for the geological data and information of outcrops, and to Torkhild Rasmussen at Luleå University of Technology for help in creating maps of outcrops. Two anonymous reviewers are gratefully acknowledged for constructive reviews that improved the quality of the manuscript.

Appendix A. Supplementary data

Supplementary data associated with this article can be found, in the online version, at https://doi.org/10.1016/j.precamres.2018.08.019.

References

Abrajevitch, A., Van der Voo, R., 2010. Incompatible Ediacaran paleomagnetic directions suggest an equatorial geomagnetic dipole hypothesis. Earth Planet. Sci. Lett. 293 (1–2), 164–170.
Bingen, B., Nordgulen, Ø., Viola, G., 2008. A four-phase model for the Sveconorwegian orogeny, SW Scandinavia. Nor. Geol. Tidsskr. 88, 43–72.
Bingen, B., Solli, A., 2009. Geochronology of magmatism in the Caledonian and Sveconorwegian belts of Baltica: synopsis for detrital zircon provenance studies. Norw. J. Geol. 89, 267–290.
Bogdanova, S.V., Page, L.M., Skridlaite, G., Taran, L.N., 2001. Proterozoic tectonothermal history in the western part of the East European Craton: $^{40}Ar/^{39}Ar$ geochronological constraints. Tectonophysics 339, 39–66.
Bogdanova, S., Gorbatschev, R., Skridlaite, G., Soesoo, A., Taran, L., Kurlovich, D., 2015. Trans-Baltic Palaeoproterozoic correlations towards the reconstruction of supercontinent Columbia/Nuna. Precambr. Res. 259, 5–33.
Boyden, J.A., Müller, R.D., Gurnis, M., Torsvik, T.H., Clark, J.A., Turner, M., Ivey-Law, H., Watson, R.J., Cannon, J.S., 2011. Next-generation plate-tectonic reconstructions using GPlates. Geoinformatics 9, 5–114.
Brander, L., Söderlund, U., 2009. Mesoproterozoic (1.47–1.44 Ga) orogenic magmatism in Fennoscandia; Baddeleyite U-Pb dating of a suite of massif-type anorthosite in S. Sweden. Int. J. Earth Sci. (Geologische Rundschau) 98, 499–516.
Brown, L.L., McEnroe, S.A., 2004. Palaeomagnetism of the Egersund-Ogna anorthosite, Rogaland, Norway, and the position of Fennoscandia in the Late Proterozoic. Geophys. J. Int. 158 (2), 479–488.
Brown, L.L., McEnroe, S.A., 2012. Paleomagnetism and magnetic mineralogy of Grenville metamorphic and igneous rocks, Adirondack Highlands, USA. Precambr. Res. 212, 57–74.
Brown, L.L., McEnroe, S.A., 2015. 916 Ma pole for southwestern Baltica: Palaeomagnetism of the Bjerkreim-Sokndal layered intrusion, Rogaland igneous complex, southern Norway. Geophys. J. Int. 203 (1), 567–587.
Buchan, K.L., Ernst, R.E., 2016. Giant circumferential dyke swarms on Earth: Possible analogues of coronae on Venus and similar features on Mars. Acta Geol. Sin. (English Edition) 90 (sup.1), 186–187.
Buchan, K.L., Ernst, R.E., 2018. A giant circumferential dyke swarm associated with the High Arctic Large Igneous Province (HALIP). Gondwana Res. 58, 39–57.
Butler, R.F., 1992. Paleomagnetism: Magnetic Domains to Geologic Terranes Vol. 319 Blackwell Scientific Publications, Boston.
Bylund, G., 1985. Palaeomagnetism of middle Proterozoic basic intrusives in central Sweden and the Fennoscandian apparent polar wander path. Precambr. Res. 28 (3-4), 283–310.
Bylund, G., Elming, S.Å., 1992. The Dala dolerites, central Sweden, and their palaeomagnetic signature. GFF 114 (1), 143–153.
Cawood, P.A., Pisarevsky, S.A., 2006. Was Baltica right-way-up or upside-down in the Neoproterozoic? J. Geol. Soc. 163 (5), 753–759.
Christoffel, C., Connelly, J.N., Åhäll, K.-I., 1999. Timing and characterization of recurrent pre-Sveconorwegian metamorphism and deformation in the Varberg-Halmstad region of SW Sweden. Precambr. Res. 98, 173–195.
Dalziel, I.W., 1997. Neoproterozoic-Paleozoic geography and tectonics: Review, hypothesis, environmental speculation. Geol. Soc. Am. Bull. 109 (1), 16–42.
Day, R., Fuller, M., Schmidt, V.A., 1977. Hysteresis properties of titanomagnetites: Grain-size and compositional dependence. Phys. Earth Planet. Inter. 13 (4), 260–267.
Denyszyn, S.W., Davis, D.W., Halls, H.C., 2009. Paleomagnetism and U-Pb geochronology of the Clarence Head dykes, Arctic Canada: Orthogonal emplacement of mafic dykes in a large igneous province. Can. J. Earth Sci. 46 (3), 155–167.
Dunlop, D.J., 2002. Theory and application of the Day plot (Mrs/Ms versus Hcr/Hc) 1. Theoretical curves and tests using titanomagnetite data. J. Geophys. Res.: Solid Earth 107 (B3).
Elming, S.Å., Pesonen, L.J., Leino, M.A.H., Khramov, A.N., Mikhailova, N.P., Krasnova, A.F., Merlanen, S., Bylund, G., Terho, M., 1993. The drift of the Fennoscandian and Ukrainian shields during the Precambrian: Aapalaeomagnetic analysis. Tectonophysics 223 (3–4), 177–198.
Elming, S.Å., Pisarevsky, S.A., Layer, P., Bylund, G., 2014. A palaeomagnetic and $^{40}Ar/^{39}Ar$ study of mafic dykes in southern Sweden: A new Early Neoproterozoic key-pole for the Baltic Shield and implications for Sveconorwegian and Grenville loops. Precambr. Res. 244, 192–206.
Ernst, R.E., Buchan, K.L., 1998. Arcuate dyke swarms associated with mantle plumes on Earth: Implications for Venusian coronae. Lunar and Planetary Science Conference #29, Houston, Texas, Abstract #1021.
Ernst, R.E., Desnoyers, D.W., Head, J.W., Grosfils, E.B., 2003. Graben-fissure systems in Guinevere Planitia and Beta Regio (264°-312°E, 24°-60°N), Venus, and implications for regional stratigraphy and mantle plumes. Icarus 164 (2), 282–316.
Evans, D.A.D., 2009. The palaeomagnetically viable, long-lived and all-inclusive Rodinia supercontinent reconstruction. Geological Society, London, Special Publications 327 (1), 371–404.
Gaál, G., Gorbatschev, R., 1987. An outline of the Precambrian evolution of the Baltic Shield. Precambr. Res. 35, 15–52.
Gower, C.F., Kamo, S., Krogh, T.E., 2008. Indentor tectonism in the eastern Grenville Province. Precambr. Res. 167, 201–212.
Hellström, F.A., Johansson, Å., Larson, S.Å., 2004. Age and emplacement of late Sveconorwegian monzogabbroic dykes, SW Sweden. Precambr. Res. 128 (1), 39–55.
Hrouda, F., 1982. Magnetic anisotropy of rocks and its application in geology and geophysics. Surv. Geophys. 5 (1), 37–82.
Hyodo, H., Dunlop, D.J., 1993. Effect of anisotropy on the paleomagnetic contact test for a Grenville dike. J. Geophys. Res. Solid Earth 98 (B5), 7997–8017.
Jaffey, A.H., Flynn, K.F., Glendenin, L.E., Bentley, W.T., Essling, A.M., 1971. Precision measurement of half-lives and specific activities of ^{235}U and ^{238}U. Phys. Rev. C 4 (5), 1889–1906.
Johansson, L., Johansson, Å., 1990. Isotope geochemistry and age relationships of mafic intrusions along the Protogine Zone, southern Sweden. Precambr. Res. 48 (4), 395–414.
Jones, C.H., 2002. User-driven integrated software lives: "Paleomag" paleomagnetics analysis on the Macintosh. Comput. Geosci. 28 (10), 1145–1151.
Kirschvink, J.L., 1980. The least-squares line and plane and the analysis of palaeomagnetic data. Geophys. J. Int. 62 (3), 699–718.

Kirschvink, J.L., Kopp, R.E., Raub, T.D., Baumgartner, C.T., Holt, J.W., 2008. Rapid, precise, and high sensitivity acquisition of paleomagnetic and rock magnetic data: Development of a low noise automatic sample changing system for superconducting rock magnetometers. Geochem. Geophys. Geosyst. 9 (5).
Knight, M.D., Walker, G.P., 1988. Magma flow directions in dikes of the Koolau Complex, Oahu, determined from magnetic fabric studies. J. Geophys. Res. Solid Earth 93 (B5), 4301–4319.
Tauxe, L., 2005. Inclination flattening and the geocentric axial dipole hypothesis. Earth Planet. Sci. Lett. 233 (3–4), 247–261.
Mäkitie, H., Data, G., Isabirye, E., Mänttäri, I., Huhma, H., Klausen, M.B., Pakkanen, L., Virransalo, P., 2014. Petrology, geochronology and emplacement model of the giant 1.37 Ga arcuate Lake Victoria Dyke Swarm on the margin of a large igneous province in eastern Africa. J. Afr. Earth Sc. 97, 273–296.
Meert, J.G., Torsvik, T.H., 2003. The making and unmaking of a supercontinent: Rodinia revisited. Tectonophysics 375 (1–4), 261–288.
Mertanen, S., Pesonen, L.J., Huhma, H., 1996. Palaeomagnetism and Sm-Nd ages of the Neoproterozoic diabase dykes in Laanila and Kautokeino, northern Fennoscandia. Geological Society, London, Special Publications 112 (1), 331–358.
McFadden, P.L., McElhinny, M.W., 1988. The combined analysis of remagnetization circles and direct observations in palaeomagnetism. Earth Planet. Sci. Lett. 87 (1–2), 161–172.
McFadden, P.L., McElhinny, M.W., 1990. Classification of the reversal test in palaeomagnetism. Geophys. J. Int. 103 (3), 725–729.
Möller, C., Andersson, A., Lundqvist, I., Hellström, F., 2007. Linking deformation, migmatite formation and zircon U-Pb geochronology in polymetamorphic orthogneisses, Sveconorwegian Province, Sweden. J. Metamorph. Geol. 25, 727–750.
Muxworthy, A.R., McClelland, E., 2000. Review of the low-temperature magnetic properties of magnetite from a rock magnetic perspective. Geophys. J. Int. 140 (1), 101–114.
Patchett, P.J., Bylund, G., 1977. Age of Grenville belt magnetisation: Rb-Sr and palaeomagnetic evidence from Swedish dolerites. Earth Planet. Sci. Lett. 35 (1), 92–104.
Pesonen, L.J., Klein, R., 2013. Paleomagnetism of some Proterozoic sediments and diabases, South Sweden. Abstract in XXVI Geofysiikan Päivät 2013, 93–96.
Pesonen, L.J., Mertanen, S., Veikkolainen, T., 2012. Paleo-Mesoproterozoic supercontinents – A paleomagnetic view. Geophysica 48 (1–2), 5–47.
Piper, J.D., Smith, R.L., 1980. Palaeomagnetism of the Jotnian lavas and sediments and post-Jotnian dolerites of central Scandinavia. GFF 102 (2), 67–81.
Pisarevsky, S.A., Wingate, M.T., Powell, C.M., Johnson, S., Evans, D.A., 2003. Models of Rodinia assembly and fragmentation. Geological Society, London, Special Publications 206 (1), 35–55.
Pisarevsky, S.A., Bylund, G., 2006. Palaeomagnetism of 935 Ma mafic dykes in southern Sweden and implications for the Sveconorwegian Loop. Geophys. J. Int. 166 (3), 1095–1104.
Poorter, R.P.E., 1975. Palaeomagnetism of Precambrian rocks from southeast Norway and south Sweden. Phys. Earth Planet. Inter. 10 (1), 74–87.
Li, Z.X., Bogdanova, S.V., Collins, A.S., Davidson, A., De Waele, B., Ernst, R.E., Fitzsimons, I.C.W., Fuck, R.A., Gladkochub, D.P., Jacobs, J., Karlstrom, K.E., 2008. Assembly, configuration, and break-up history of Rodinia: A synthesis. Precambr. Res. 160 (1), 179–210.
Ludwig, K.R., 2003. User's manual for isoplot 3.00, a geochronlogical toolkit for microsoft excel. Berkeley Geochronl. Cent. Spec. Publ. 4, 25–32.
Lundmark, A.M., Lamminen, J., 2016. The provenance and setting of the Mesoproterozoic Dala Sandstone, western Sweden, and paleogeographic implications for southwestern Fennoscandia. Precambr. Res. 275, 197–208.
Ripa, M., Mellqvist, C., Ahl, M., Andersson, D., Bastani, M., Delin, H., Kübler, L., Nyston, P., Persson, L., Thelander, T., 2012. Bedrock map Western part of the county Dalarna, scale 1: 250 000. Sveriges Geologiska Undersökning K 382.
Rochette, P., Jackson, M., Aubourg, C., 1992. Rock magnetism and the interpretation of anisotropy of magnetic susceptibility. Rev. Geophys. 30 (3), 209–226.
Rose, I., Buffett, B., 2017. Scaling rates of true polar wander in convecting planets and moons. Phys. Earth Planet. Inter. 273, 1–10.
Slagstad, T., Roberts, N.M., Marker, M., Røhr, T.S., Schiellerup, H., 2013. A non-collisional, accretionary Sveconorwegian orogen. Terra Nova 25 (1), 30–37.
Söderlund, U., Johansson, L., 2002. A simple way to extract baddeleyite (ZrO_2). Geochem. Geophys. Geosyst. 3 (2).
Söderlund, U., Möller, C., Andersson, J., Johansson, L., Whitehouse, M., 2002. Zircon geochronology in polymetamorphic gneisses in the Sveconorwegian orogen, SW Sweden: ion microprobe evidence for 1.46-1.42 and 0.98-0.96 Ga reworking. Precambr. Res. 113, 193–225.
Söderlund, U., Patchett, P.J., Vervoort, J.D., Isachsen, C.E., 2004a. The ^{176}Lu decay constant determined by Lu-Hf and U-Pb isotope systematics of Precambrian mafic intrusions. Earth Planet. Sci. Lett. 219 (3), 311–324.
Söderlund, P., Söderlund, U., Möller, C., Gorbatschev, R., Rodhe, A., 2004b. Petrology and ion microprobe U-Pb chronology applied to a metabasic intrusion in southern Sweden: A study on zircon formation during metamorphism and deformation. Tectonics 23 (5).
Söderlund, U., Isachsen, C.E., Bylund, G., Heaman, L.M., Patchett, P.J., Vervoort, J.D., Andersson, U.B., 2005. U-Pb baddeleyite ages and Hf, Nd isotope chemistry constraining repeated mafic magmatism in the Fennoscandian Shield from 1.6 to 0.9 Ga. Contrib. Miner. Petrol. 150 (2), 174–194.
Solyom, Z., Lindqvist, J.E., Johansson, I., 1992;al. The geochemistry, genesis, and geotectonic setting of Proterozoic mafic dyke swarms in southern and central Sweden. GFF 114 (1), 47–65.
Squyres, S.W., Janes, D.M., Baer, G., Bindschadler, D.L., Schubert, G., Sharpton, V.L., Stofan, E.R., 1992. The morphology and evolution of coronae on Venus. J. Geophys. Res. Planets 97 (E8), 13611–13634.
Stacey, J.T., Kramers, J.D., 1975. Approximation of terrestrial lead isotope evolution by a two-stage model. Earth Planet. Sci. Lett. 26 (2), 207–221.
Stearn, J.E.F., Piper, J.D.A., 1984. Palaeomagnetism of the Sveconorwegian mobile belt of the Fennoscandian Shield. Precambr. Res. 23 (3–4), 201–246.
Stofan, E.R., Head, J.W., 1990. Coronae of Mnemosyne Regio: Morphology and origin. Icarus 83 (1), 216–243.
Van der Voo, R., 1990. The reliability of paleomagnetic data. Tectonophysics 184 (1), 1–9.
Veikkolainen, T., Pesonen, L.J., 2014. Palaeosecular variation, field reversals and the stability of the geodynamo in the Precambrian. Geophys. J. Int. 199 (3), 1515–1526.
Veikkolainen, T.H., Biggin, A.J., Pesonen, L.J., Evans, D.A., Jarboe, N.A., 2017. Advancing Precambrian palaeomagnetism with the PALEOMAGIA and PINT ($_{QPI}$) databases. Sci. Data 4, 170068.
Wahlgren, C.H., Cruden, A.R., Stephens, M.B., 1994. Kinematics of a major fan-like structure in the eastern part of the Sveconorwegian orogen, Baltic Shield, south-central Sweden. Precambr. Res. 70 (1–2), 67–91.
Walderhaug, H.J., Torsvik, T.H., Eide, E.A., Sundvoll, B., Bingen, B., 1999. Geochronology and palaeomagnetism of the Hunnedalen dykes, SW Norway: Implications for the Sveconorwegian apparent polar wander loop. Earth Planet. Sci. Lett. 169 (1), 71–83.
Walderhaug, H.J., Torsvik, T.H., Halvorsen, E., 2007. The Egersund dykes (SW Norway): A robust early Ediacaran (Vendian) palaeomagnetic pole from Baltica. Geophys. J. Int. 168 (3), 935–948.
Weil, A.B., Geissman, J.W., Ashby, J.M., 2006. A new paleomagnetic pole for the Neoproterozoic Uinta Mountain Supergroup, central Rocky Mountain states, USA. Precambr. Res. 147 (3), 234–259.
Wen, B., Evans, D.A., Li, Y.X., 2017. Neoproterozoic paleogeography of the Tarim Block: An extended or alternative “missing-link” model for Rodinia? Earth Planet. Sci. Lett. 458, 92–106.
Wen, B., Evans, D.A., Wang, C., Li, Y.X., Jing, X., 2018. A positive test for the Greater Tarim Block at the heart of Rodinia: Mega-dextral suturing of supercontinent assembly. Geology 46 (8), 687–690.
Zijderveld, J.D.A., 1967. AC demagnetization of rocks: analysis of results. MethodsPaleomagnet 3, 254.

Precambrian Research 320 (2019) 484–485

Contents lists available at ScienceDirect

Precambrian Research

journal homepage: www.elsevier.com/locate/precamres

Corrigendum

Corrigendum to "Paleomagnetism, magnetic anisotropy and U-Pb baddeleyite geochronology of the early Neoproterozoic Blekinge-Dalarna dolerite dykes, Sweden" [Precambrian Res. 317 (2018) 14–32]

Zheng Gong[a,*], David A.D. Evans[a], Sten-Åke Elming[b], Ulf Söderlund[c,d], Johanna M. Salminen[e]

[a] Department of Geology and Geophysics, Yale University, 210 Whitney Avenue, New Haven, CT 06511, USA
[b] Department of Civil, Environmental and Natural Resources Engineering, Luleå University of Technology, SE-971 87 Luleå, Sweden
[c] Department of Geology, Lund University, SE-223 62 Lund, Sweden
[d] Swedish Museum of Natural History, Laboratory of Isotope Geology, SE-104 05 Stockholm, Sweden
[e] Department of Geosciences and Geography, University of Helsinki, Helsinki 00014, Finland

The authors regret that the incorrect version of Table 3 and Fig. 12 appeared in the paper. The corrected Table 3 and Fig. 12 are presented below. In Table 2, Group A mean direction should be Dec = 128.8°, Inc = 39.6°, α_{95} = 6.5°, and Group B mean direction should be Dec = 127.6°, Inc = 65.4°, α_{95} = 9.7°. These changes do not affect any main conclusion of the paper. The authors would like to apologize for any inconvenience caused.

Table 3
Paleomagnetic poles used to constrain the paleogeographic reconstruction of Baltica and Laurentia at ca. 1000–850 Ma.

#	Paleomagnetic Pole	Dec (°)	Inc (°)	α_{95} (°)	k	N/n	Plat (°N)	Plon (°E)	A_{95} (°)	S (°)	|λ| (°)	Age (Ma)	1	2	3	4	5	6	7	Q	Reference
Baltica																					
1	Hunnedalen dykes	294.0	−75.0	6.0	115	6/69	−41.0	222.0	10.5	13.4	61.8	848 ± 27[a]; 855 ± 59[b]	1	1	1	0	1	0	1	5	Walderhaug et al. (1999)
2	Egersund-Ogna anorthosite	325.9	−80.1	4.9	73	13/69	−42.1	200.4	9.0	17.3	70.8	900[c]	1	1	1	0	0	0	1	4	Brown and McEnroe (2004)
3	Egersund anorthosite	–	–	–	–	76/–	−43.5	213.7	3.6	–	–	900[c]	0	1	1	0	0	0	1	3	Stearn and Piper (1984); Walderhaug et al. (1999)
4	Rogaland Igneous Complex	269.0	−72.0	11.0	49	5/24	−45.9	238.4	18.2	19.4	57.0	869 ± 14[a]	1	0	1	1	0	0	1	4	Walderhaug et al. (2007)
5	Bjerkreim-Sokndal intrusion	303.4	−73.5	3.7	24	66/354	−35.9	217.9	6.0	26.1	59.4	916[c]	1	1	1	0	1	0	1	5	Brown and McEnroe (2015)
6	Mean 951–935 Ma Baltica pole	308.8	−39.6	6.5	42	12/116	−2.6	239.6	5.8	10.8	22.5	951–935[d]	1	1	1	1	1	1	1	7	This study
7	971 Ma BDD dykes VGP	307.6	−65.4	14.2	68	4/36	−27.0	230.4	14.9	13.0	47.5	971 ± 7[d]	1	0	1	0	1	1	1	5	This study
8	Laanila-Ristijärvi dykes	355.5	−40.0	17.5	51	3/7	−2.1	212.2	16.4	9.0	22.8	1042 ± 50[b]	0	0	1	1	1	0	0	3	Mertanen et al. (1996)
9	Bamble Intrusion mean	–	–	–	–	–	3.0	217.0	15.0	–	–	1100–1040	0	1	1	0	0	0	0	2	Meert and Torsvik (2003)
Laurentia																					
10	Adirondack microcline gneisses	289.2	−62.8	7.6	29	14/80	−18.4	151.1	10.5	22.0	44.2	960[c]	1	1	1	0	0	1	1	5	Brown and McEnroe (2012)

(*continued on next page*)

DOI of original article: https://doi.org/10.1016/j.precamres.2018.08.019
* Corresponding author.

https://doi.org/10.1016/j.precamres.2018.10.013
Received 15 October 2018; Accepted 30 October 2018
Available online 02 November 2018

Table 3 (*continued*)

#	Paleomagnetic Pole	Dec (°)	Inc (°)	α_{95} (°)	k	N/n	Plat (°N)	Plon (°E)	A_{95} (°)	S (°)	|λ| (°)	Age (Ma)	1	2	3	4	5	6	7	Q	Reference
11	Adirondack metamorphic anorthosites and other rocks	283.9	−67.3	7.7	28	14/68	−25.1	149.0	11.6	24.3	50.1	970[c]	1	1	1	0	0	1	1	5	Brown and McEnroe (2012)
12	Adirondack fayalite granites	297.0	−75.8	3.9	199	8/40	−28.4	132.7	6.9	10.2	63.2	990[c]	1	1	1	0	0	1	1	5	Brown and McEnroe (2012)

Note: Dec = declination, Inc = inclination, α_{95} = radius of 95% confidence cone of the mean direction, k = precision parameter, N/n = number of site/sample, Plat/Plon = paleomagnetic pole latitude/longitude, A_{95} = radius of 95% confidence cone of the paleomagnetic pole, S = angular dispersion of VGPs, |λ| = absolute value of paleolatitude, Q = sum of quality criteria (Van der Voo, 1990).

[a] Ar-Ar biotite ages.
[b] Sm-Nd whole rock ages.
[c] Cooling ages.
[d] U-Pb baddeleyite ages.

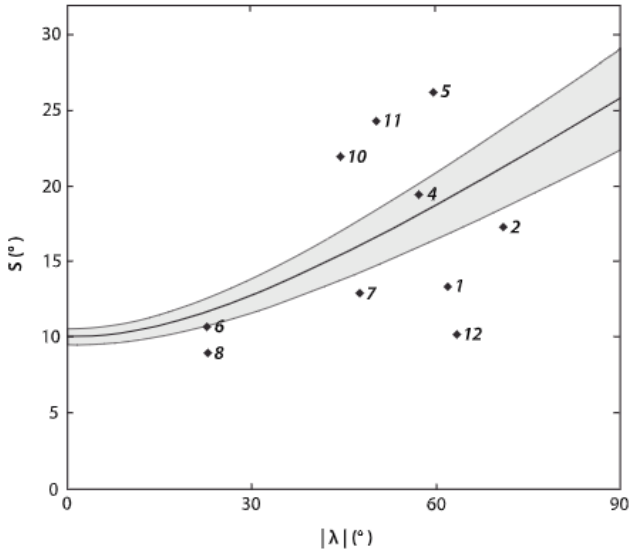

Fig. 12.